An Experimental Investigation of the Surface Tension of Seawater

by

Kishor Govind Nayar

B.Tech, Mechanical Engineering
Indian Institute of Technology Bombay, Mumbai, 2012

Submitted to the Department of Mechanical Engineering
in partial fulfillment of the requirements for the degree of

Master of Science in Mechanical Engineering

at the

MASSACHUSETTS INSTITUTE OF TECHNOLOGY

June 2014

Signature redacted

Author ....
Department of Mechanical Engineering
May 9, 2014

Signature redacted

Certified by..... .....
John H. Lienhard V
Collins Professor of Mechanical Engineering
Thesis Supervisor

Signature redacted

Accepted by ....
David E. Hardt
Chairman, Committe on Graduate Students

An Experimental Investigation of the Surface Tension of Seawater

by

Kishor Govind Nayar

Submitted to the Department of Mechanical Engineering
on May 9, 2014, in partial fulfillment of the
requirements for the degree of
Master of Science in Mechanical Engineering

Abstract

Surface tension of seawater was measured for absolute salinities S = (20.01, 35.18, 40.49, 79.39, 121.54) g/kg across a temperature range of T = (0 - 90)°C at atmospheric pressure using the Wilhelmy plate method. The uncertainty within measurements varied between 0.04 - 0.33 mN/m with the average uncertainty being 0.12 mN/m. The experimental procedures were validated with tests conducted on ACS reagent grade water and aqueous sodium chloride solutions. A best fit correlation was developed expressing surface tension of seawater as a function of temperature and salinity. The average absolute deviation between measurements and the correlation was 0.19% while the maximum deviation was 0.60%. The surface tension of seawater was found to be comparable to within 1.37% of the surface tension of aqueous sodium chloride. The surface tension of 0.2 μm microfiltered and ultraviolet radiation treated natural seawater was found to be similar to that of laboratory prepared seawater.

Thesis Supervisor: John H. Lienhard V
Title: Collins Professor of Mechanical Engineering

Acknowledgments

I would like to first thank my advisor, Prof. John H. Lienhard V, for providing me a great deal of support and guidance over the last 2 years. I greatly appreciate the freedom he gave me in taking ownership of my work and for compassionately being there whenever I faced difficulty. I have learnt a lot working with Prof. Lienhard and I hope to emulate how effectively he handles all his responsibilities. I am very thankful for having him as my advisor.

I would like to thank Divya Panchanathan, who collaborated with me in carrying out surface tension experiments. Working with her was a great experience and I greatly appreciate the support she has given me. I would also like to thank Prof. Gareth H. McKinley for providing guidance during experimentation. I wish to also acknowledge 2 amazing undergraduate students who worked with me on this project, Meghan Nelson, who worked with me for 2 months in the summer of 2013, and Adrian Jimenez-Galindo, who has been working with me since the summer of 2013. The dedication and sincerity that both students showed was admirable. I wish to also thank Prof. Robert E. Cohen for generously allowing me to use his laboratory to conduct experiments. I am also thankful to Prof. Cohen's group for supporting the experiments. I wish to also thank Dr. Paul Brown and Prof. T. Alan Hatton for allowing me to use the rotary evaporator in their laboratory. I am very grateful to King Fahd University of Petroleoum and Minerals (KFUPM), Dhahran, Saudi Arabia, for supporting my work through the Center for Clean Water and Clean Energy at MIT and KFUPM. I wish to also thank Prof. Mostafa H. Sharqawy at KFUPM for sharing with me the raw data he had used to develop an earlier correlation for the surface tension of seawater.

I wish to thank my lab mates in the Lienhard Research Group for giving me suggestions and helping me in my work. I would like to specially thank Jaichander (Jaichu), Emily, Greg, Ronan, Leo, David, Karim, Charlene and Lige for supporting me whenever I was facing difficulties. In particular I would like to thank my dear friend, Jaichu, for putting up with me and for letting me crash at his house for power-

naps whenever I drove myself to exhaustion. I also greatly appreciate Greg for taking the time to help me prioritize aspects of my work.

I am grateful to my dear friend and BE writing coach/angel [:)], Alison Takemura, for helping me write better and for supporting me as I wrote my thesis. I would also like to thank Suhrid Deshmukh for being a great friend. I am also thankful to my friends at the Art of Living Foundation: Alison, Annelies, Anuj, Gaurav, Jackie, Jayen, Neha, Richa, Sareena and Swami, for being there for me these past 2 years. I would also like to thank my coaches at Landmark Worldwide for distinguishing the perfectionist streak in me and help me get past it.

I would like to thank my mom, my dad and my sister for showering me with love and for encouraging me, always praying for me and giving me immense support. I wish to also thank my grandparents, my aunt and my cousins for always wishing the best for me. I am also very grateful to my uncle, Sanjeev Govindan, for giving me tips and helping me during the thesis-writing process and knocking some sense into me whenever I needed it! I feel truly blessed to have an amazing supportive family.

I am thankful to my teachers at Loyola School, Trivandrum and the Indian Institute of Technology Bombay (IITB), Mumbai for shaping my ability to learn and my thought processes. In particular, I would like to thank my Bachelors thesis advisor, Prof. Milind V. Rane, for cultivating my interest in research and the thermal sciences. I wish to also thank all my teachers at MIT and the rigorous mechanical engineering qualifying exams for giving me greater confidence in my abilities as an engineer.

I am thankful to my spiritual mentor, Sri Sri Ravi Shankar, for always reminding me that I am not alone and that I am here on the planet to serve. I look forward to serving humanity better through the development and application of technologies.

Contents

1 Introduction **17**

2 Literature Review **19**

2.1 Theory and Definitions 19

2.2 Methods 20

2.2.1 Surface Tension 20

2.2.2 Temperature 24

2.2.3 Salinity 24

2.3 Experiments and Semi-empirical fits 24

2.3.1 Sodium Chloride 24

2.3.2 Seawater 26

3 Experimentation **29**

3.1 Measurements 30

3.1.1 Surface Tension 30

3.1.2 Temperature 35

3.1.3 Salinity 39

3.2 Test Solutions 40

3.2.1 Preparation 41

3.3 Experimental Problems and Solutions 43

3.3.1 Evaporation 43

3.3.2 Condensation on the Lid 46

3.3.3 Condensation on the Wilhelmy plate 48

3.3.4 Contamination 48
3.3.5 Contact Angle Changes due to Adsorption on Platinum Plate 48
3.4 Cleaning Protocol 50
3.5 General Procedure 51
3.6 Data Analysis 52
3.6.1 Surface Tension 53
3.6.2 Temperature 56
3.6.3 Salinity 56
3.7 Uncertainty Analysis 60
3.7.1 Surface Tension 60
3.7.2 Temperature 61
3.7.3 Salinity 61

4 Results and Discussion **65**
4.1 Validation 65
4.2 Surface Tension of ASTM Seawater 69
4.3 Comparison of Surface Tension of ASTM Seawater with Aqueous Sodium Chloride 72
4.4 Comparison of ASTM and ASCS Seawater 74
4.5 Precipitation of Sparingly Soluble Salts 76
4.6 Effect of Scale Formation 78

5 Conclusions **83**

A Experimental Data **85**

List of Figures

2-1 Wilhlemy plate method 22

2-2 Timeline showing past work on the surface tension of seawater 26

3-1 Diagram of the tensiometer 29

3-2 Photograph of the DCAT11 tensiometer 31

3-3 Photograph of the Wilhelmy plate 32

3-4 Depiction of a single measurement of surface tension. Top figure represents the first 12 seconds of recorded surface tension. Bottom figure represents the same measurement over 200 seconds. 35

3-5 Fluke 5611 Teflon thermistor and Fluke 1524 thermometer 35

3-6 Diagram of the thermistor showing its position 37

3-7 Plot of measured temperature vs time showing a static and bulk temperature measurement 38

3-8 Mettler Toledo AG204 Delta Range mass balance 39

3-9 Photograph of concentration using a rotary evaporator 42

3-10 Comparison of evaporation rates for different lid designs 44

3-11 Final design of the lid 45

3-12 Technical drawing of the lid 46

3-13 Photograph of lid with heater and insulation 47

3-14 Contact angle measurement of 35 g/kg ASTM seawater on a platinum Wilhlemy plate scaled by sea salt 50

3-15 Flame cleaning of the Wilhelmy plate 51

3-16 Plot showing surface tension measurements of ACS water at 20°C and 80°C saturating to expected values. The variation is presumed to be because of the electronic compensation mechanism in the microbalance 54

3-17 Plot showing surface tension measurements of ACS water at 20°C and 80°C after exclusion of measurements far from the saturated value . . 56

4-1 Comparison of present measurements of surface tension of pure water and aqueous sodium chloride solutions to values from literature correlations 66

4-2 Expanded uncertainty in surface tension measurements for ACS water and aqueous sodium chloride solutions 67

4-3 Deviation of surface tension measurements of ACS water and aqueous sodium chloride from the their corresponding literature correlations given by Eq. 2.11 and Eq. 2.4 68

4-4 Complete set of measurements for surface tension of ASTM seawater 69

4-5 Expanded uncertainty in surface tension measurements for ASTM seawater 70

4-6 Deviation of surface tension measurements of ASTM seawater from surface tension calculated by Eq. 4.1 71

4-7 Deviation of seawater surface tension data of Chen et al. [1] from surface tension calculated using Eq. 4.1 72

4-8 Surface tension of ASTM seawater compared with Dutcher's correlation for aqueous sodium chloride 73

4-9 Deviation of surface tension measurements of ASTM seawater from surface tension of aqueous sodium chloride calculated using Dutcher's correlation, Eq. 2.4 74

4-10 Surface tension measurements of 35.16 g/kg ASCS seawater compared with the results of the best fit correlation for ASTM seawater given in Eq. 4.1 along with a deviation band of 0.60% 75

4-11 Results of Energy Dispersive Spectrum (EDS) analysis of a sample of precipitate obtained from 35 g/kg ASCS seawater tested at $T = 80°C$ showing the presence of elemental carbon, oxygen, magnesium, sulphur, chlorine and calcium along with an scanning electron microscope (SEM) image of the analyzed sample 77
4-12 Comparison of 35 g/kg ASTM seawater under normal conditions and after 4 hours of testing at $T = 70°C$ and $80°C$ 77
4-13 Precipitates the surface of 35 g/kg ASTM and after 4 hours of testing at $T = 70°C$ and $80°C$ 78
4-14 Surface tension decreasing below the surface tension of pure water after scale formation on the test beaker 79
4-15 Surface tension decreasing below the surface tension of pure water after scale formation on the test beaker for $T > 50°C$ 80

List of Tables

3.1 Parameters of tensiometer specified in SCAT 11 33

3.2 Summary of test solutions 42

3.3 Summary of contact angles tests 49

3.4 Comparison of calculated and measured salinities for experiments conducted on ASTM seawater with the deviations for intermediate salinity measurements depicted in bold 59

A.1 Measurements for ACS water 85

A.2 Measurements for aqueous sodium chloride 86

A.3 Measurements for ASTM seawater 87

A.4 Measurements for ASCS seawater 88

Nomenclature

Roman symbols

Cl	Chlorinity [g/kg]
f	Correction factor
F	Force [mN]
g	Acceleration due to gravity [m^2/s]
k	Coverage factor
m	Mass [g]
n	Final number of measurements at a test temperature
N	Total number of measurements at a test temperature
p	Wetted perimeter [mm]
P_{vap}	Vapor pressure [kPa]
s	Sample standard deviation
S	Absolute salinity [g/kg]
S_K	Knudsen salinity [g/kg]
S_P	Practical salinity [g/kg]
S_R	Reference salinity [g/kg]

se Standard error

t time [hr]

T Temperature, ITS-90 scale [°C]

T_K Temperature, ITS-90 scale [K]

T_{27} Temperature, ITS-27 scale [°C]

u Uncertainty

u_c Combined uncertainty

U Overall uncertainty

x Mole fraction

Greek symbols

α Confidence interval

Δ Difference

γ Surface tension [mN/m]

ρ Density [kg/m^3]

θ Contact angle [°]

Subscripts

NaCl Sodium chloride

s Molten salt

soln Solution

solv Solvent

sw Seawater

w Water

Chapter 1

Introduction

Surface tension of seawater is an important thermodynamic property for accurately designing seawater desalination technologies where vapor transfer occurs across a liquid-air or liquid-vapor interface. For example, surface tension plays a key role in tailoring the non-wettability of membranes in Membrane Distillation (MD) [2] and in optimizing heat and mass transfer in packed beds and falling film evaporators for Humidification Dehumidification (HDH) desalination and Multi-Effect Distillation (MED) respectively [3]. While there is data on the surface tension of seawater in the oceanographic range of temperature and salinities (T = 0 - 40°C and S = 0 - 40 g/kg) from previous literature [1, 4, 5], there is no data in the standard operating range for thermal desalination (T = 40 - 100°C and S = 40 - 120 g/kg). It is this gap in literature that this work seeks to fill.

The problem of a lack of data or inaccurate data in the thermal desalination range is encountered in other seawater properties as well. In the desalination industry and research community, these gaps are worked around by approximating seawater as an aqueous sodium chloride solution of equivalent concentration and using known properties of sodium chloride [6–11]. The same approach can be used for surface tension as well. Past experiments have shown that surface tension of seawater and aqueous sodium chloride are similar at low temperatures ($T \approx 13$°C) [12]. However it is not clear whether this is the case at elevated temperatures ($T > 50$°C) where sparingly soluble salts like calcium sulphate ($CaSO_4$), calcium carbonate ($CaCO_3$),

magnesium carbonate ($MgCO_3$) and magnesium hydroxide ($Mg(OH)_2$) are known to precipitate [13].

The objective of this thesis is to determine experimentally the surface tension of seawater as a function of temperature and salinity across both the oceanographic and thermal desalination ranges (T = 0 - 90°C and S = 0 - 120 g/kg) at atmospheric pressure. This work further explores the accuracy of approximating seawater as an aqueous solution of sodium chloride especially at elevated temperatures where precipitation of sparingly soluble salts is known to occur. Furthermore the effect of trace organic substances and heavy metals on the surface tension of seawater was explored through a comparison between laboratory prepared substitute seawater and treated actual ocean water.

The thesis is structured in the following manner. First a literature review is presented in Chapter 2 on surface tension theory, experimental methods and past experiments conducted on seawater. The experimental procedure used to measure surface tension in this work is presented next in Chapter 3 while the results are discussed in Chapter 4. The last chapter, Chapter 5 contains the conclusions of the thesis.

Chapter 2

Literature Review

Divya Panchanathan contributed to this chapter.

2.1 Theory and Definitions

Surface tension is a property of a liquid/solid which arises due to unbalanced intermolecular forces acting on molecules at an interface. It can be viewed as a contractile force which acts at the perimeter of the surface to shrink the surface area. Surface tension may also be viewed as equivalent to the energy required to create a unit area of new surface. To create a new surface, molecular forces of attraction need to be overcome. These attractive forces are weak Van der Waals forces in organic liquids and are much stronger electrostatic forces arising from hydrogen bonds for pure water. Thus pure water has a higher surface tension than organic liquids.

The surface tension of a pure substance is closely related to its P-V-T equation of state [14], with the surface tension between a pure liquid and its vapor decreasing with temperature and reaching a value of zero at the critical point of the liquid. Empirically it has been established that the surface tension of pure substances vary with temperature proportional to $(1 - \frac{T_K}{T_c})^{11/9}$ [15] where T_K is the temperature of the pure substance in kelvin and T_c is the critical temperature of the pure substance.

The surface tension of aqueous electrolyte solutions including seawater increases with salinity [16]. This is because ions strongly prefer to be hydrated in the bulk of

the solution rather than migrate to the surface. This leads to a thin layer of water at the surface which is largely devoid of ions but strongly held by the hydration shells of the ions in the bulk of the solution. These forces are stronger than hydrogen bonds in pure water. The effect increases with increase in salinity. Onsager and Sameras [17] explained this for low salinities using the concept of electrostatic "image forces". New theories have also been developed that includes other effects to explain this for high salinities as well [18].

Absolute salinity (S) of seawater is defined by Millero et al. [19] as the "mass fraction of dissolved materials in seawater". The absolute salinity of seawater is experimentally difficult to determine and has been approximated historically by different salinity scales such as Knudsen salinity (S_K), Chlorinity (Cl), Practical Salinity (S_P) and the most recent reference salinity (S_R). The detailed descriptions of these as well as equations to convert between each salinity scale can be found in Millero et al. [19]. A description of the current ITS-90 temperature scale and historical temperature scales such as the ITS-27, IPTS-48 and the IPTS-68 scale along with the equations to convert between them is given by Preston-Thomas [20].

2.2 Methods

2.2.1 Surface Tension

The methods for measuring surface tension can be classified into the following four categories based on the measured parameter [21]:

1. interfacial force
2. interfacial pressure
3. capillary effect
4. drop shape

Interfacial force based methods. The Wilhelmy plate and Du Nuoya ring methods are two popular interfacial forced based methods for measuring surface tension. In

this approach, a probe is first immersed slowly into the liquid. The liquid then wets the probe and climbs its way above the interface. The weight of the liquid column above the interface is supported by the surface tension force acting at the three phase interface created by the liquid, air and probe. This force is then transmitted to and measured by a sensitive microbalance attached to the probe. The force measurement can be measured either through a 'static' approach or through a 'detachment' approach. In the 'static' approach, the probe is immersed in the liquid and held stationary, and force resulting from the interface is measured. In the 'detachment' approach, the probe is first immersed in the liquid and subsequently pulled out. The force required to detach the probe from the interface is then measured by the microbalance. In both approaches, surface tension is calculated as a function of the force measured by the microbalance, contact angle at the interface and the geometry of the probe.

In the case of the Wilhelmy plate method, the probe used is a thin flat plate. This method allows for both 'static' and 'detachment' approaches. Surface tension for this method is given by Eq. 2.1:

$$\gamma = F/(p^*\cos(\theta)) \tag{2.1}$$

where F is the force measured, p is the wetted perimeter of the plate and θ is the contact angle between the plate and the liquid.

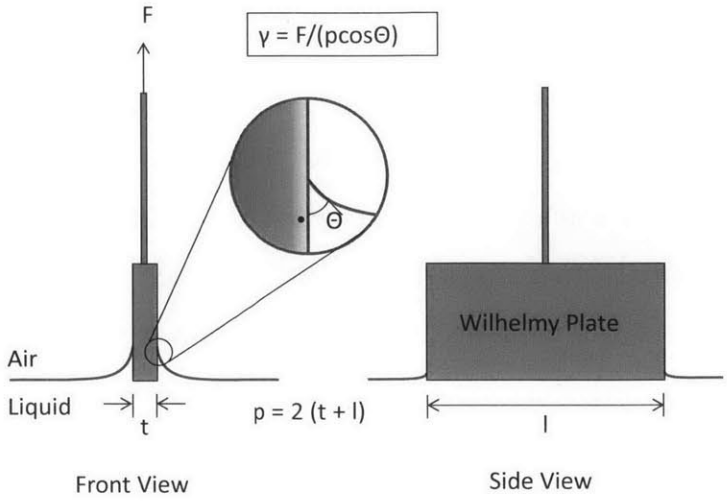

Figure 2-1: Wilhlemy plate method

In the case of the Du Nuoya ring method, the probe is a ring and the relationship between surface tension and the force measured by the microbalance is given by Eq. 2.2:

$$\gamma = F/(p^*\cos(\theta)^*f) \tag{2.2}$$

Unlike the Wilhelmy plate method, the Du Nuoya ring method requires a correction factor (f) to compensate for the weight of excess liquid lifted by the ring when it is pulled out of the liquid. The correction factor is itself a function of density of the liquid, force measured by the microbalance and the dimensions of the ring. To measure surface tension accurately, the force exerted by the interface around the ring must be uniform. This is achieved only as long as the plane of the ring is parallel to the liquid interface. Thus great care must be taken in handling the ring to prevent the ring from deforming.

Interfacial pressure based methods The maximum bubble pressure method is a popular method for measuring surface tension that uses pressure to obtain surface tension. Gas (air or nitrogen) is blown into the test solution through a tube and the pressure in the tube is measured as the gas bubble grows in the fluid. The pressure varies as the gas bubble increases in radius. The maximum pressure is recorded and

surface tension is obtained from the Young-Laplace equation given by Eq. 2.3:

$$\Delta P = \gamma * (\frac{1}{R_1} + \frac{1}{R_2}) \tag{2.3}$$

where, R_1 and R_2 are radii of curvature. The method is accurate and the measurement time is small (0.001-0.1 seconds). This method is one of the most popular methods to measure surface tension presently.

Capillary effect based methods. The capillary rise and drop volume methods are two methods that were popular for measuring surface tension. In both cases an interplay between capillary and gravity forces results in a measurable effect, height of a liquid column in the case of the capillary rise method and the volume of liquid in the drop volume method. Historically the capillary rise method has been very popular due to its simplicity and high accuracy. The standard datasets for the surface tension of several fluids were obtained using this method. However the advent of electronic data recording has caused this method to go out of fashion because the measurement of height is more difficult to automate. The method also required very fine glass capillaries to produce accurate results.

Drop shape based methods. The pendant drop and sessile drop methods are two methods where an interplay between capillary and gravity forces cause a drop of test solution to assume a particular shape. Surface tension is then calculated from the shape of the drop. With the advent of image processing, state-of-the-art instruments solve for surface tension by fitting the shape of the drop to the theoretical curves.These methods are not suitable for surface tension measurements at elevated temperatures. This is because the small size of the drop with respect to the environment causes high heat transfer at the interface. Thus accurate readings would require maintaining the environment to be in equilibrium with the solution both in temperature and concentration (i.e, the environment is saturated with the vapor state of the solvent to prevent mass transfer across the interface). The method is however quite useful for obtaining surface tension measurements at near ambient temperatures due to the low heat and mass transfer rates at ambient conditions.

2.2.2 Temperature

A review of different methods for measuring temperature such as platinum resistance temperature devices (RTD), thermocouples, and thermistors along with the working principles and typical accuracies is given by Childs et al. [22] and Beckwith et al. [23].

2.2.3 Salinity

The absolute salinity of seawater is typically estimated using salinity meters that measure the electrical conductivity of seawater which is well correlated with salinity [19]. While this approach is accurate up to $S = 42$ g/kg, uncertainties in the relationship between salinity and electrical conductivity are higher beyond 42 g/kg. Thus experiments in the past that conducted experiments on high salinity ($S > 42$ g/kg) seawater obtained salinity by evaporating seawater of a known salinity and measuring the final mass of the concentrated seawater [24, 25].

2.3 Experiments and Semi-empirical fits

2.3.1 Sodium Chloride

Numerous experiments have been conducted over the last 100 years on the surface tension of aqueous sodium chloride solutions [12, 26–30]. For the purpose of validating the experimental procedure, the most recent and accurate semi-empirical fit for aqueous sodium chloride developed by Dutcher et al. in 2010 was used [31]. The Dutcher model used 194 surface tension measurements of sodium chloride spread across a temperature range of T = (-10.02 - 200)°C salinity S = (0 - 550) g/kg from 11 sources in the literature. The model could predict surface tension across a wide spectrum of concentration - from infinite dilution up to molten salt. The average absolute error between the original measurements and the results of the fit was 0.72%.

Dutcher's model calculates surface tension as a weighted average of contributions to surface tension from pure water (γ_w) and molten salt (γ_s),

$$ln(\gamma_{\mathrm{NaCl}}(T_K)) = x_{\mathrm{w}} \ln(\gamma_{\mathrm{w}}(T_K) + x_{\mathrm{s}} F_{\mathrm{ws}}(T_K)) + x_{\mathrm{s}} \ln(\gamma_s(T_K) + x_{\mathrm{w}} F_{\mathrm{sw}}(T_K)) \quad (2.4)$$

where x_{w} is the mole fraction of pure water in the solution and x_{s} is the mole fraction of the salt in the solution and,

$$\gamma_{\mathrm{s}} = c_1 + c_2 T_K \quad (2.5)$$

$$F_{\mathrm{ws}}(T_K) = a_{\mathrm{ws}} + b_{\mathrm{ws}} T_K \quad (2.6)$$

$$F_{\mathrm{sw}}(T_K) = a_{\mathrm{sw}} + b_{\mathrm{sw}} T_K \quad (2.7)$$

where $a_{\mathrm{ws}} = 232.54$ mN/m, $b_{\mathrm{ws}} = -0.245$ mN/m-K, $a_{\mathrm{sw}} = -140.52$ mN/m, $b_{\mathrm{sw}} = 0$ mN/m-K, $c_1 = 191.16$ mN/m, $c_2 = -0.07188$ mN/m-K and T_K is in kelvin.

One of the main advantages of this model was that it accounted for changes in the variation of surface tension with concentration at low and high salt concentrations. However, it is important to note that all the fitted data were not taken for the same ranges of temperature and concentrations, and therefore some extrapolation is involved in some cases. We used this as our reference data curve for validating our water and aqueous sodium chloride data due to the low error observed over the application range.

2.3.2 Seawater

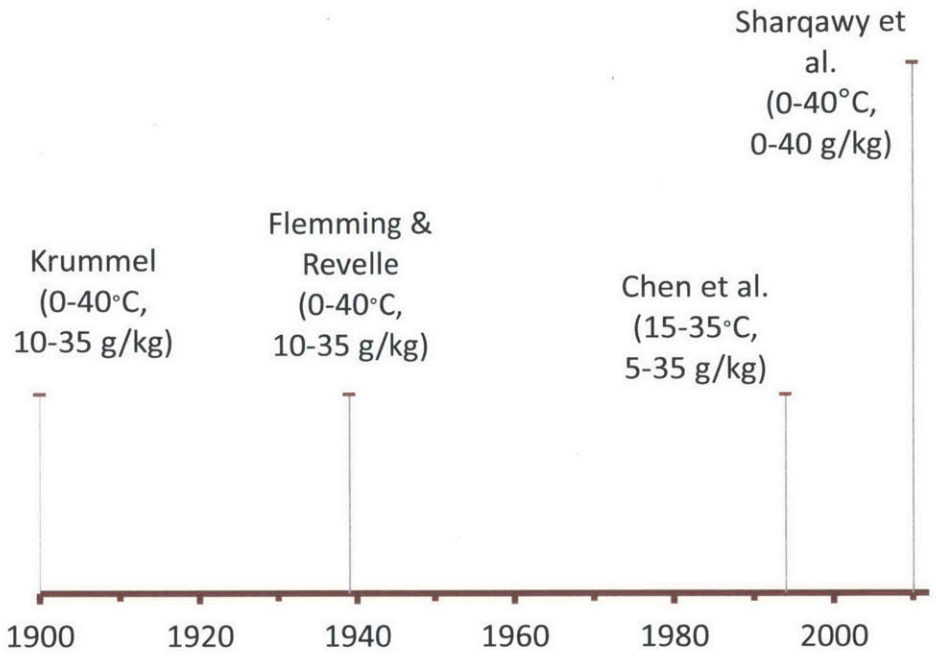

Figure 2-2: Timeline showing past work on the surface tension of seawater

In the last hundred years, there has been only two experimental investigations of the surface tension of seawater. Krummel [12] in 1900 obtained the surface tension of seawater to increase the accuracy of hydrometers used for measuring the specific gravity of seawater especially at low temperatures. An early variant of the bubble pressure method originally developed by Gustav Jaeger [32] was used by Krummel for measuring surface tension. Surface tension measurements were carried out on five samples of seawater with Kndusen salinities [33] S_{K} = (7.73, 13.00, 15.82, 24.96 and 34.90) g/kg and six samples of aqueous sodium chloride with salinites S_K = (0.52, 3.80, 5.00, 7.00, 9.00 and 10.00) g/kg with the temperature being varied from 11 to 13°C. Krummel subseqently tabulated the difference in surface tension between the combined dataset and the surface tension for pure water at the same measured temperature as calculated from a prior correlation. The difference was then fit linearly

with Knudsen salinity to give Eq. 2.8:

$$\gamma_{sw} = 77.09 \ - 0.1788T_{27} + 0.0221S_K \tag{2.8}$$

where, γ_{sw} is surface tension in mN/m, T_{27} is temperature in Celsius as defined by the ITS-27 historical temperature scale mentioned in Section 2.1 and S_K is Kundsen salinity in g/kg. Krummel stated a deviation between measurements and the correlation of 0.04 mN/m. While Krummel did not clearly state the uncertainty in measurements, inspection of the dataset revealed that there was atleast an uncertainty of 0.03 - 0.38% in Krummel's measurements.

Fleming and Revelle [4] subsequently in 1939 published an improved correlation by combining Krummel's data for surface tension of seawater with updated measurements of the surface tension of pure water. The result is given in Eq. 2.9:

$$\gamma_{sw} = 75.64 - 0.144T_{27} + 0.399Cl \tag{2.9}$$

where, γ_{sw} is surface tension in mN/m, T_{27} is temperature in Celsius as defined by the ITS-27 temperature scale and Cl is Chlorinity in g/kg.

New experiments to determine the surface tension of seawater were conducted by Chen et al. [1] in 1994 using the maximum bubble pressure method. Experiments were conducted on natural seawater with practical salinties S_P = (4.965, 15.220, 20.006, 25.062, 29.464 and 34.486) g/kg over a temperature range of 15 to 35°C . For this study, the original solution used was filtered seawater of salinity S_P = 34.486 g/kg from the North Pacific in Japan. Test solutions of lower salinites were prepared by diluting the original solution with water. The test solution temperature was held stable to within 0.005°C and was measured using a Beckmann thermometer with a precision of 0.001°C. While the uncertainty in surface tension measurement was not explicitly mentioned, it can be inferred to be at least 0.15 mN/m from the stated precision (0.2%) of the bubble pressure tensiometer. Surface tension measurements

were then fit as a function of temperature and salinity to Eq. 2.10:

$$\gamma_{sw} = 75.59 - 0.13476\,T + 0.021352\,S_P - 0.00029529\,S_P T \tag{2.10}$$

where, γ_{sw} is surface tension in mN/m, T is temperature in Celsius in the current ITS-90 temperature scale and S_P is practical salinity in g/kg. The absolute average deviation between the correlation and measurements was 0.07 mN/m while the maximum deviation was 0.12 mN/m.

Sharqawy et al. [5] in 2010 developed a new correlation by fitting the data from Krummel and Chen to a modified form of the Szykowski equation. Sharqawy had observed that the correlations developed previously did not yield the surface tension of pure water as salinity approached 0 g/kg. Past seawater data was subsequently normalized with the IAPWS standard equation for the surface tension of pure water [34] given by Eq. 2.11:

$$\gamma_w = 235.8 \left(1 - \frac{T_K}{647.096}\right)^{1.256} \left[1 - 0.625 \left(1 - \frac{T_K}{647.096}\right)\right] \tag{2.11}$$

where, γ_w is the surface tension in mN/m and T_K is temperature in kelvin in the current ITS-90 temperature scale and a new correlation for surface tension of seawater was developed. This is given by Eq. 2.12:

$$\gamma_{sw} = \gamma_w \left[1 + (0.000226\,T + 0.00946)\,\ln(1 + 0.0331\,S)\right] \tag{2.12}$$

where, γ_{sw} is surface tension in mN/m, T is temperature in Celsius in the current ITS-90 temperature scale and S is absolute salinity in g/kg. A maximum deviation of 0.28% between the data and correlation was reported. It must be noted that the analysis of the data from Krummel had revealed uncertainties as high as 0.38% and that the IAPWS correlation for the surface tension of pure water itself has an uncertainly of 0.4% at low temperatures. Thus, the actual maximum deviation from Sharqawy's correlation could be higher than 0.68%.

Chapter 3

Experimentation

In this section, the final methods selected for measuring surface tension, temperature and salinity are first presented. Subsequently, the methodology for preparing test solutions, the cleaning protocol used, the experimental difficulties faced and the solution to the difficulties are presented along with data and uncertainty analysis.

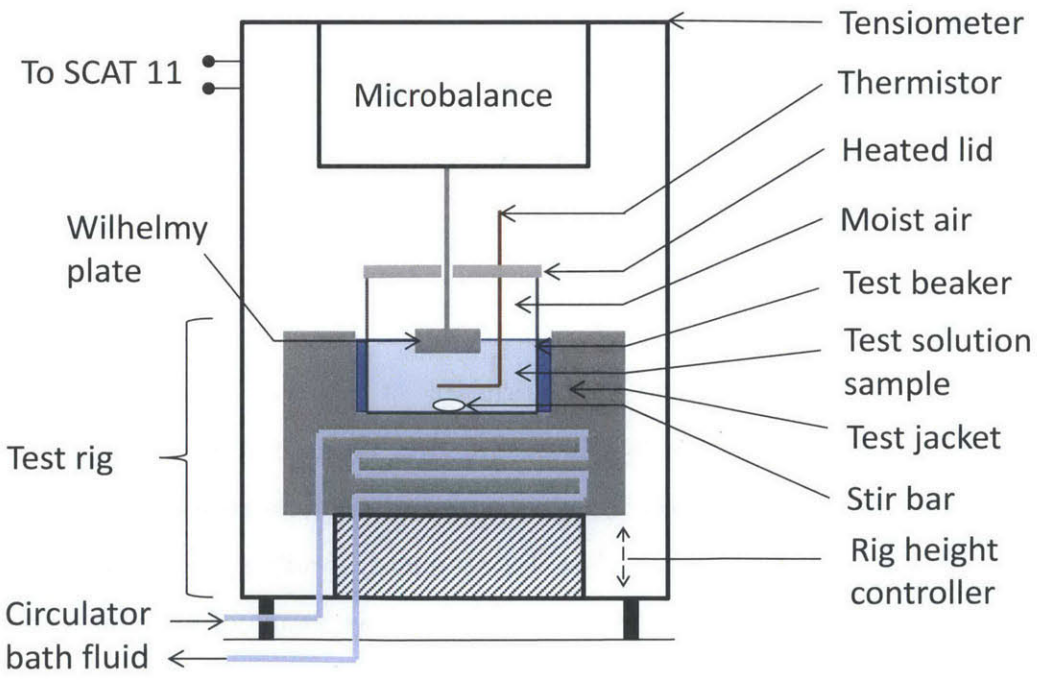

Figure 3-1: Diagram of the tensiometer

3.1 Measurements

3.1.1 Surface Tension

Surface tension was measured using the Wilhelmy plate method. This method was selected over other methods because it:

1. is very accurate (≈ 0.1 mN/m)
2. allows for the test solution sample to be maintained at a stable temperature
3. is a direct measurement without correction factor (when used with a platinum Wilhelmy plate)
4. allows for the interface to be near a state of equilibrium

The Wilhelmy plate method was implemented using a Dataphysics DCAT11 [35, 36] tensiometer that could measure surface tension to a resolution of 0.001 mN/m. The tensiometer can be thought to be consisting of three main parts: a fixed microbalance at the top, a Wilhelmy plate attached to the microbalance, and a movable test rig at the bottom.

The force exerted on the plate by the interface is transmitted to and measured by the microbalance. The microbalance is very sensitive and can measure weights to a resolution of 0.01 mg. The central weighing module of the microbalance uses a "monolith" weighing technology developed by the German balance manufacturer Sartorius. The technology worked on the principle of "electrodynamic compensation" which is described in great detail by Chan et al. [37]. The microbalance is calibrated to a built in 100 g $\pm$ 0.15 mg reference mass using an internal algorithm. The reference mass in the microbalance fit the class E2 standard specified by the International Organization of Legal Metrology (OIML) [38]. This approach of internal calibration is a common feature of high accuracy weigh cells [39]. The tensiometer is internally calibrated at the beginning of every day of testing.

Figure 3-2: Photograph of the DCAT11 tensiometer

While the reference mass of the microbalance is well defined, to make accurate weight or force measurements, the acceleration due to gravity (g) must also be specified. This was calculated by the Cohen group from the exact global position of the tensiometer (latitude, longitude and altitude from sea-level) obtained using a global positioning system. The 'g' value calculated was 9.803878 m^2/s. This gives a resolution of force measurement of 0.001 mN/m.

To maintain a zero contact angle between the Wilhelmy plate and the test solution sample, a platinum Wilhelmy plate (length 19.9 mm, width 10 mm and thickness 0.2 mm) was selected. This is because platinum has a high surface energy which allows it to be completely wetted by liquids. Eq. 2.1 then simplifies as:

$$\gamma = F/p \tag{3.1}$$

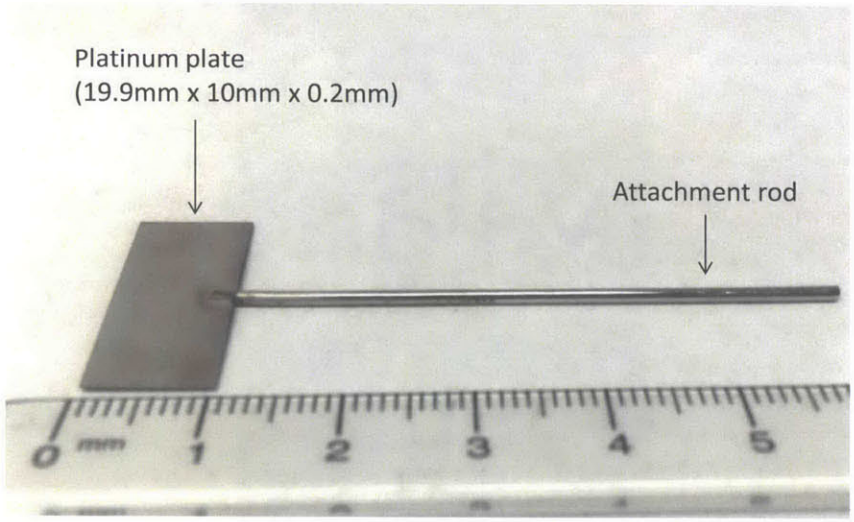

Figure 3-3: Photograph of the Wilhelmy plate

The movable test rig part of the tensiometer has a test jacket designed by the manufacturer for two purposes: to allow easy placement of the test beaker assembly containing the test solution sample and to ensure that the temperature of the jacket walls are as uniform as possible to reduce thermal gradients in the beaker and test solution sample.

The test beaker assembly consisted of a borosilicate glass test beaker (diameter 70 mm and height 40 mm) [40], the test solution sample, a stir bar and a heated lid which is described in detail in Section 3.3. Air made moist by vapor evaporating from the test solution sample filled the space between the heated lid and the sample. The dimensions of the test solution sample was sufficiently large enough (diameter 70 mm) when compared with plate dimensions (19.90 mm) to avoid wall effects.

The operation of the tensiometer was controlled by a computer using the SCAT11 software developed by Dataphysics. The software allows for specific parameters like the speed of the rig movement, the minimum weight measured to detect a surface, the samples of surface tension measured per second and the immersion depth to be specified. The settings that were used for each of these are given in Table 3.1.

Table 3.1: Parameters of tensiometer specified in SCAT 11

Parameter	Value	Units
Motor speed	0.5	mm/s
Surface detection threshold	4.00	mg
Samples/second	5.00	Hz
Immersion depth	3.00	mm

Measurement of surface tension

At the beginning of each measurement, the microbalance records the weight of the Wilhelmy plate, tares itself, and then the test rig slowly starts moving up towards the Wilhelmy plate. The SCAT11 software detects when the Wilhelmy plate makes contact with the interface and causes the plate to be immersed further up to a preset depth. Subsequently the rig moves down and the plate is brought back to the level of the interface so that the only force experienced by the plate is the force arising from surface tension. The immersion is done for complete wetting of the plate and also to compensate for the effect of advancing and receding contact angles. Once the plate has come back to the interface, the recording of surface tension commences with surface tension being sampled every 0.2 seconds.

A single surface tension measurement (γ_i) is then obtained by taking an average value of a sample of the recorded values of surface tension. The uncertainty in a single surface tension measurement (σ_{γ_i}) is given by the standard deviation of the sample.

The SCAT 11 software allows for two approaches to select a sample for averaging:

1. Standard deviation approach: Surface tension can be recorded till the last 50 data points have a standard deviation less than a desired value. The average of these last 50 data points constitutes a single surface tension measurement (γ_i) with the target deviation (σ_{γ_i}).

2. Time interval approach: Surface tension can be recorded for a set duration and the average of recordings over a pre-set range of time can be taken to constitute a single surface tension measurement (γ_i). The standard deviation of recordings

in this period of time is the deviation in the single surface tension measurement (σ_{γ_i})

Typically for surface tension measurements conducted at room temperature, Approach 1 is used. However, Approach 1 can lead to significant errors at elevated temperatures ($T > 50°C$) because of the problem of condensation of water droplets on the Wilhelmy plate and the attachment rod during the recording of surface tension. This effect caused the measured value of surface tension to rise with time as more water droplets condense onto the Wilhelmy plate and attachment rod. At times it was also found to cause sharp drops in measured surface tension when the drops fall off of the Wilhelmy plate. To avoid this problem and to keep a uniform procedure across all experiments, Approach 2 was used for averaging surface tension recordings. Surface tension recordings were averaged for 10 seconds between the 1st and 11th seconds. This short time frame significantly reduced the effect condensation had on the measurement. Furthermore, recordings of surface tension were found to be quite stable within this interval. Recordings before t = 1 seconds was not used because of an impulse response occurring in the measurement when the test-rig stops moving at time t = 0 seconds. The impulse response and the effect condensation of droplets have on measurement can be seen in Fig. 3-4.

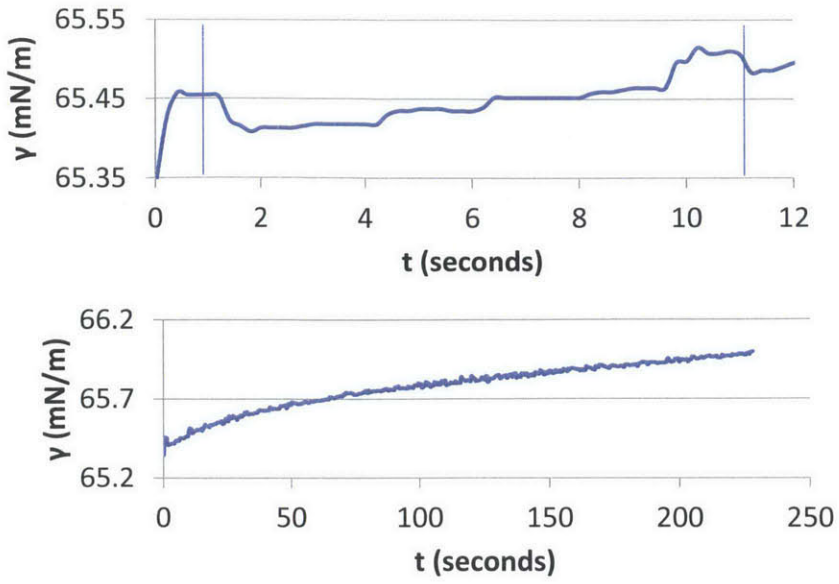

Figure 3-4: Depiction of a single measurement of surface tension. Top figure represents the first 12 seconds of recorded surface tension. Bottom figure represents the same measurement over 200 seconds.

3.1.2 Temperature

Measurement

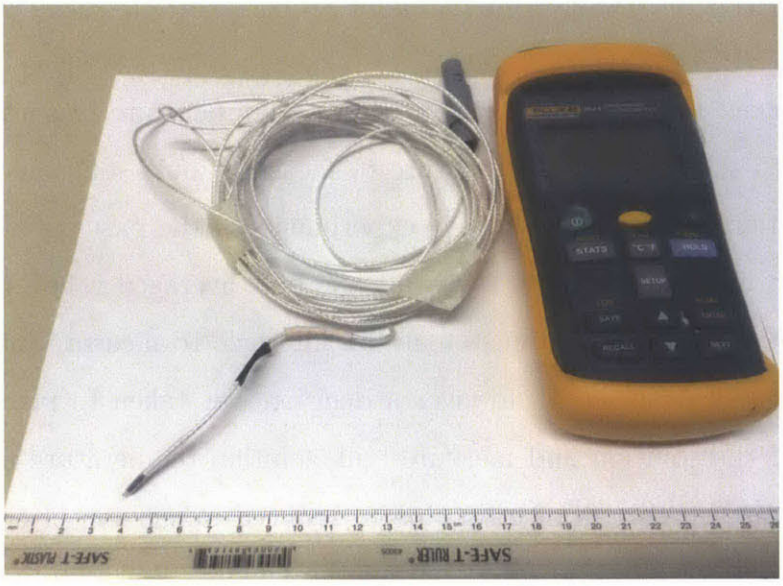

Figure 3-5: Fluke 5611 Teflon thermistor and Fluke 1524 thermometer

To measure the temperature of the test solution sample accurately, a 5611 Teflon thermistor probe [41] and a model 1524 reference thermometer [42] from the company Fluke was used. The probe was selected over other thermocouples, resistance temperature detectors (RTDs) because of its:

1. high accuracy (0.01°C) in the range of measurement (0-100°C)
2. small size (diameter 3 mm and sensor length of 13 mm) and thus low self-heating errors
3. ability to measure tempeature accurately even at low immersion depths
4. impervious Teflon coating which reduced the risk of cross contamination between experiments and contamination risks from corrosion.

The 5611 thermistor probe was calibrated across the full range of temperature (0-100°C) by the company to measurement standards traceable to the National Institute of Standards and Technology (NIST) and was in compliance with the standards ISO/IEC 17025 [43] and ANSI/NCSL Z450-1-1994 [44]. The 1524 reference thermometer was also calibrated by Fluke to measurement standards traceable to NIST and complied with calibration requirements in part 2 of ANSI/NCSL Z450-1-1994 [44].

An important question related to measuring temperature in surface tension experiments is to select which temperature to measure: bulk solution temperature or the interface temperature. Only a few experiments in the past have considered this question, with most experiments reporting the bulk averaged values of temperature. The option of placing the thermistor at the interface to measure interface temperature was initially considered; however a decision was taken to place the probe at the bottom of the solution and measure bulk solution temperature for two reasons. First, there was a high risk of error due to reduced immersion of the probe in the former case; and, second, a lot of experimental difficulty was seen in positioning the thermistor at the level of the interface, especially when interface level is susceptible to changes occurring due to evaporation.

The position of the thermistor is depicted with relevant dimensions in Fig. 3-6. It was ensured that in all experiments, that 55 mm of the probe measured from the top of the lid is immersed vertically into the beaker. This was length found to allow the complete immersion of the probe in the test solution sample. A depth of approximately 22 mm of the test solution sample was maintained to ensure that the height of the surface of the test solution sample is less than the height to which the test jacket extends. This was done to limit the temperature fluctuations at the solution surface.

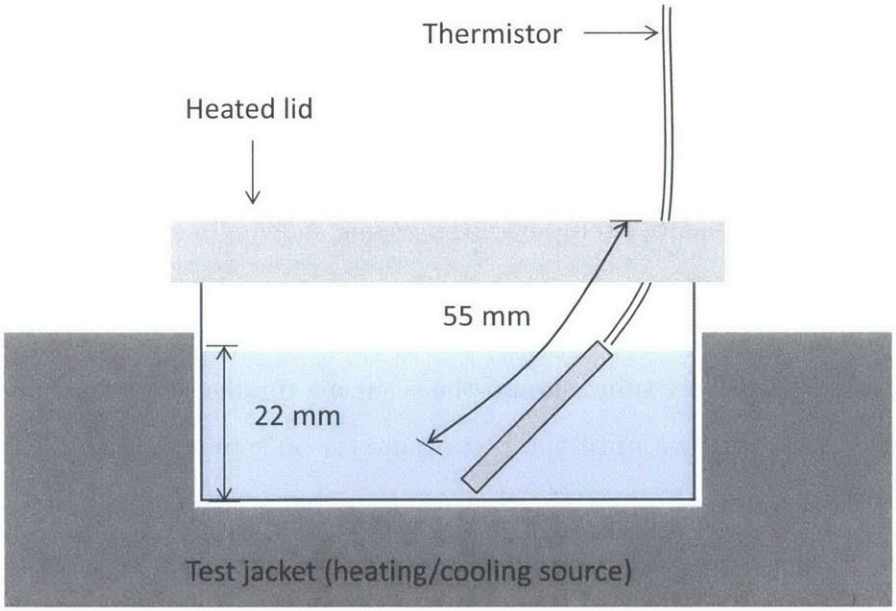

Figure 3-6: Diagram of the thermistor showing its position

To better quantify the thermal gradients in the test solution sample, two temperature measurements were taken for every surface tension measurement (γ_i): a static temperature measurement (T_{s_i}) obtained for an unstirred test solution and a bulk temperature measurement (T_{b_i}) obtained after stirring the test solution using a stir bar. While the measurement of the static temperature was straightforward, the bulk temperature measurement was more nuanced and is described with the help of temperature data depicted in Fig. 3-7:

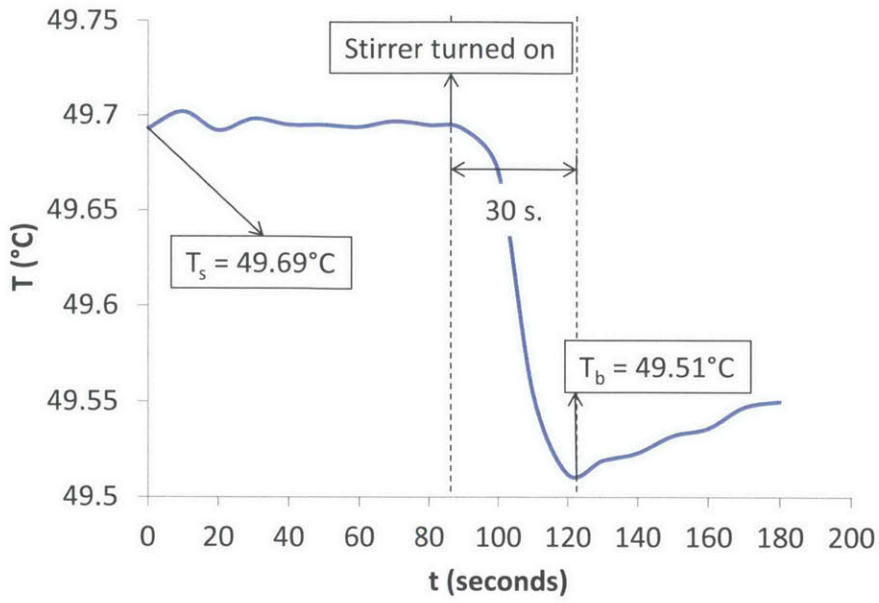

Figure 3-7: Plot of measured temperature vs time showing a static and bulk temperature measurement

The stirring of the test solution and the resulting mixing causes a sharp change in the measured temperature until the instantaneous bulk temperature of the solution is reached. The time required for this point to be reached was generally around 30 seconds. This point was read visually with the help of a temperature vs. time plotting feature of the 1524 thermometer. To limit the maximum error arising from the visual measurement, measurements were taken within 45 seconds. The maximum uncertainty observed using this approach was 0.03°C.

Control

To maintain a stable test solution sample temperature a Julabo F12-ED refrigerated and heating circulator [45] was used. To ensure smooth operation of the circulator across the test range of 0 to 100°C, a 50% by weight mixture of glycol in water was used as the circulator working fluid. The temperature control mechanism of the circulator could achieve a temperature stability within 0.03°C.

3.1.3 Salinity

The absolute salinity of test solutions was measured indirectly using a mass based approach. All solutions used for testing were sourced from original solutions of known absolute salinities. Whenever a solution was diluted or concentrated, its mass was measured to obtain the absolute salinity of the new solution. This approach of measuring mass was preferred over measuring electrical conductivity because of uncertainties in seawater electrical conductivity beyond salinities of 40 g/kg and temperatures of 40°C. Furthermore, the accuracy of the mass based approach was higher and it was also a non-invasive way to measure salinity. The latter consideration was important because of a concern that frequent immersion and removal of a conductivity probe could contaminate the test solution sample.

Figure 3-8: Mettler Toledo AG204 Delta Range mass balance

For measuring mass, a Mettler Toledo AG204 Delta Range mass balance [46] (referred hereafter as Mass Balance A), a Mettler Toledo PG2002-S mass balance (referred hereafter as Mass Balance B) [47] and a Ohaus Scout II SC2040 [48] mass balance (referred hereafter as Mass Balance C) were used. Mass Balance A had a

measurement resolution of 0.001 g for a maximum capacity of 210 g. Mass Balance B had a measurement resolution of 0.01 g for a maximum capacity of 2100 g. Mass Balance C had a measurement resolution of 0.01 g for a maximum capacity of 400 g. While the mass balances were calibrated by the manufacturer, additional accuracy tests were conducted with the help of reference weights. Reference weights (0.3078848 g) from TA instruments were used to cross-check the accuracy of Mass Balances A and B. The analysis showed that actual accuracy of mass balance A was 0.001 g while that of mass balance B was 0.1 g. The accuracy of Mass Balance C was then verified to be 0.01 g with the help of the more accurate Mass Balance A.

Mass Balances A and C were used primarily to measure the salinity of test solution samples ($\approx$ 60 g) used for testing on the tensiometer, while Mass Balance B was used exclusively to prepare large quantities of test solutions ($\approx$ 500 g).

3.2 Test Solutions

To meet the objectives described in Chapter 1, surface tension experiments were carried out on ACS[1] reagent grade water [49] (referred hereafter as ACS seawater), aqueous sodium chloride solutions, seawater solutions prepared from the ASTM D1141 standard for substitute ocean water without heavy metals [50] (referred hereafter as ASTM seawater) and seawater solutions from the Atlantic Seawater Conductivity Standard [51] (referred here as ASCS seawater).

ACS reagent grade water and aqueous sodium chloride solutions were used to validate the experimental procedure used. ASTM seawater solutions were used to generate a standard data set for the surface tension of seawater across a temperature range of $T = 0$ - 90°C and salinity range of $S = 0$ to 120 g/kg. For this purpose, ASTM seawater was preferred over other seawater standards such as the IAPSO standard [52] and ASCS seawater because ASTM seawater is a laboratory preparation that lacks organic content which may affect the accuracy of surface tension measurements. IAPSO and ASCS seawater by comparison is natural seawater from the Atlantic which

[1] American Chemical Society

is microfiltered through a 0.2 μm membrane, treated with ultraviolet radiation and calibrated to a standard salinity. While the organic content in IAPSO and ASCS seawater is low by virtue of the treatment process, trace organics still do exist along with heavy metals. ASCS seawater solutions were used to verify whether the results obtained from ASTM seawater could be applied to properly treated natural seawater.

3.2.1 Preparation

ACS reagent grade water was procured from Sigma-Aldrich and directly used for testing.

Aqueous sodium chloride solutions were prepared from an original solution of 5M (246.38 g/kg) Bioultra aqueous sodium chloride solution [53] purchased from Sigma Aldrich. The original solution was diluted with ACS water to obtain test solutions of salinities S = (39.99, 80.20 and 120.01) g/kg. The required quantity of test solution ($\approx$ 250 g) was prepared by adding smaller quantities of ($\approx$ 60 g) original solution and ACS water. The smaller quantities could be measured upto an accuracy of 0.001 g using Mass Balance A. Accounting for a maximum overall error of 0.01 g in weight in the final test solution, a preparation accuracy in salinity of 0.01 g/kg was obtained for aqueous sodium chloride.

ASTM seawater solutions were prepared from an original solution of ASTM D1141 standard seawater without heavy metals ($S = 35.18 \pm 0.02$ g/kg) [54] purchased from the Ricca Chemical Company. ASTM seawater solutions with salinities S = (40.49, 79.39 and 121.54) g/kg were prepared by concentrating the ASTM D1141 solution by evaporating solvent under reduced pressure at $T = 55$°C using a Buchi R-210 Rotovapor rotary evaporator [55]. The temperature of the seawater solution being concentrated was carefully selected to inhibit precipitation of sparingly soluble salts. However, some amount of precipitation was still observed even under these conditions. ASTM seawater of salinity $S = 20.01$ g/kg was prepared by diluting the standard solution with ACS water. Test solutions of ASTM seawater were prepared in large quantities ($\approx$ 500 g) to reduce the effect of preparation errors. The mass of these solutions were measured using analytical Mass Balance B which had an accuracy of

0.1 g. The resulting uncertainty in salinity from preparation was was 0.01 g/kg for test solutions of salinities S = (20.01, 40.49 and 79.39) g/kg and was 0.05 g/kg for the test solution of salinity S = 121.54 g/kg. The difference was because the 121.54 g/kg solution was prepared in batches of 250 g.

ASCS seawater ($S = 35.16$ g/kg) procured from OSIL was directly used for testing. The error in salinity quoted by OSIL for ASCS seawater was 0.07 g/kg.

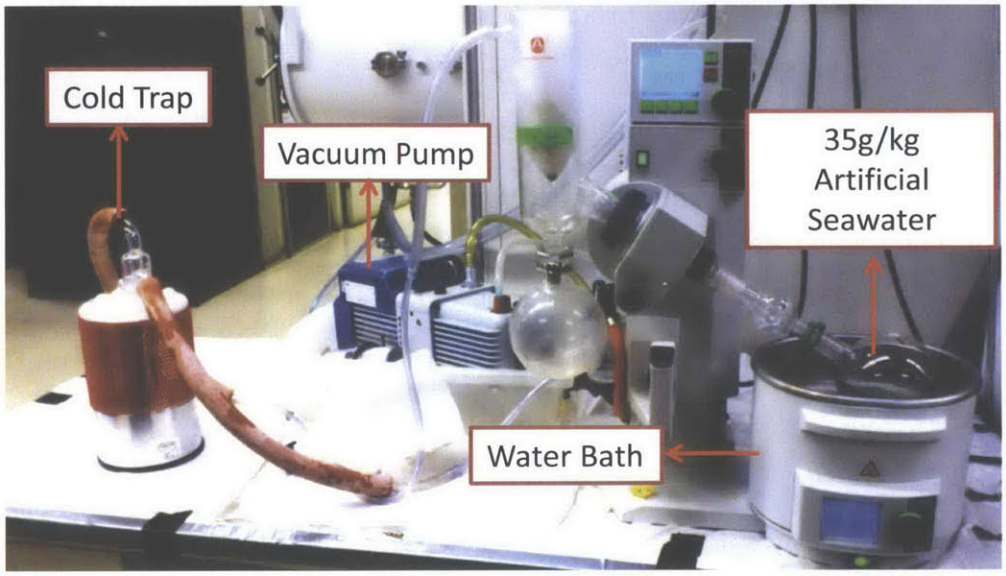

Figure 3-9: Photograph of concentration using a rotary evaporator

Table 3.2: Summary of test solutions

Test Solutions	**Original Solution**	**Salinities Prepared (g/kg)**	**Error (g/kg)**
ACS water	ACS reagent grade water	-	-
NaCl	5M Tissue-culture grade NaCl (246.38 g/kg)	39.99, 80.20, 120.01	0.01
ASTM seawater	ASTM D 1141 Substitute Ocean (35.18 g/kg)	20.01, 35.18, 40.49, 79.39, 121.54	0.02 - 0.06
ASCS seawater	Atlantic Seawater Conductivity Standard (35.16 g/kg)	35.16	0.07

3.3 Experimental Problems and Solutions

While the tensiometer used had a high precision of 0.001 mN/m, obtaining accurate repeatable measurements required overcoming several sources of errors and experimental difficulties. These as well as their solutions are discussed in this section.

3.3.1 Evaporation

One of the main experimental difficulties faced was of evaporation of the test solution sample at elevated temperatures ($T > 50°C$). It affected the repeatability of measurements by affecting the equilibrium of the interface, creating thermal gradients within the test solution sample and more importantly by affecting the salinity of the sample. The effect on salinity was particularly significant because of the small mass of the test solution sample (60 g). For example at 120 g/kg salinity, a solvent loss of 1 g translates into a salinity increase of 1.7%. To inhibit solvent loss through evaporation,it was decided to design a special lid to be placed on the test beaker.

To further quantify the effect of evaporation and to explore the effectiveness of different lid designs, evaporation tests were conducted. Approximately 60 g of deionized water was taken in a beaker, and different lid designs were fixed to it. The assembly was then heated to approximately 80°C. Four lid designs were compared: a control case without a lid, a lid with a 30x10 mm hole (dimensions selected for easy movement of the Wilhelmy plate), a simple glass cover without sealing (to see the effect of sealing) and lastly a sealed lid with a 2 mm hole corresponding to the diameter of the Wilhelmy plate rod (to test the combined effect of a small orifice and sealing). Tests were conducted over approximately two hours and average evaporation rates were calculated for each case. Results showed that without the presence of a lid, the rate of solvent loss was as high as 15 g/hr. The lid with a 30x10 mm hole gave similar results as the control case - meaning that the vapor pressure difference established by the 30x10 mm hole was not significant enough to reduce vapor diffusion. The unsealed lid performed better than the control case allowing for a solvent evaporation rate of 4 g/hr. The best performing design was the sealed lid with a 2 mm hole which allowed

a solvent loss rate of only 1 g/hr. For the purpose of designing the experiment, this was important because it placed an upper bound on how much evaporation could be be limited to. The results of the tests is summarized Fig. 3-10.

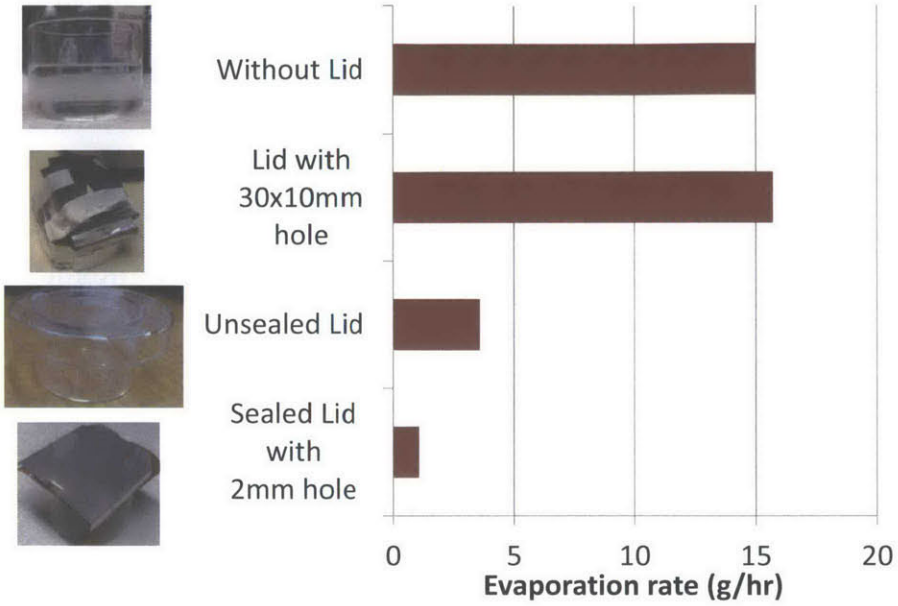

Figure 3-10: Comparison of evaporation rates for different lid designs

Lid Design and Fabrication

To allow a 2 hour window for conducting high temperature experiments, it was decided that the lid could not have an orifice diameter bigger than 2 mm. To allow for the easy insertion and removal of the Wilhelmy plate, a 30 x 10 mm hole was cut into the lid for the easy insertion of the Wilhelmy plate (length 20 mm, thickness 0.2 mm) into the moist air part of the test beaker. To suppress evaporation while still allowing for easy insertion and free relative movement of the Wilhelmy plate, special doors were designed to control the area of the hole exposed to the environment. When fully open, the doors exposed the hole completely allowing the plate section of the Wilhelmy plate to completely enter. When fully closed, the doors create a 2 mm orifice at the center of the hole for the rod section of the Wilhelmy plate to stick out of the lid and allow for the free movement of the plate. To reduce the space

occupied by the lid, the doors were designed to slide over the top surface of the lid along the plane of the hole instead of more common designs where doors open in a plane different from the plane of the hole. To keep the weight of the assembly of the lid, test beaker and test solution sample below the upper limit of the mass balance (215 g) used for measuring salinity, aluminum was the material of choice for the lid. Aluminum was also the preferred choice because its high conductivity allowed the lid to maintain a more uniform temperature. This was important because the lid had to be uniformly heated to a temperature close to the liquid temperature to reduce condensation of solvent on the lid as well as natural convection within the moist air above the test solution sample. This aspect is described in greater detail in Section 3.3.2. The final design is shown in Fig. 3-11.

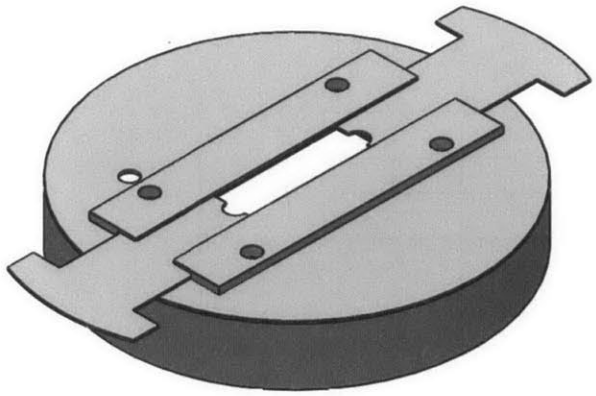

Figure 3-11: Final design of the lid

Subsequently a prototype of the lid made of acrylic was laser-cut and tested out. The tolerances were improved further and the lid was fabricated in 3 sections:

1. an aluminum cylindrical shell (outer diameter 76 mm and inner diameter 70.1 mm)

2. a flat aluminum top surface with precise cuts for thermistor probe and the Wilhelmy plate to enter (diameter 76 mm and thickness 0.5 mm)

3. doors for insertion and removal of the Wilhelmy plate and guide rails for guiding the doors.

The cylindrical portion was machined on a lathe from an aluminum cylindrical shell. A thin groove was cut into the top end of the cylindrical shell to leave space for the fitting of an Aramid steam seal. The seal was meant to prevent suppress leakage of vapor at the joint between the test beaker and the lid. The top piece with the desired holes, doors and guiderails was cut from a 0.5 mm aluminum sheet using a waterjet cutter. To fuse the cylindrical shell with the top surface, an adhesive was used. Brazing was not considered for this operation because the aluminum flat plate was too thin to prevent warping. The dimensions of the parts are given in Fig. 3-12.

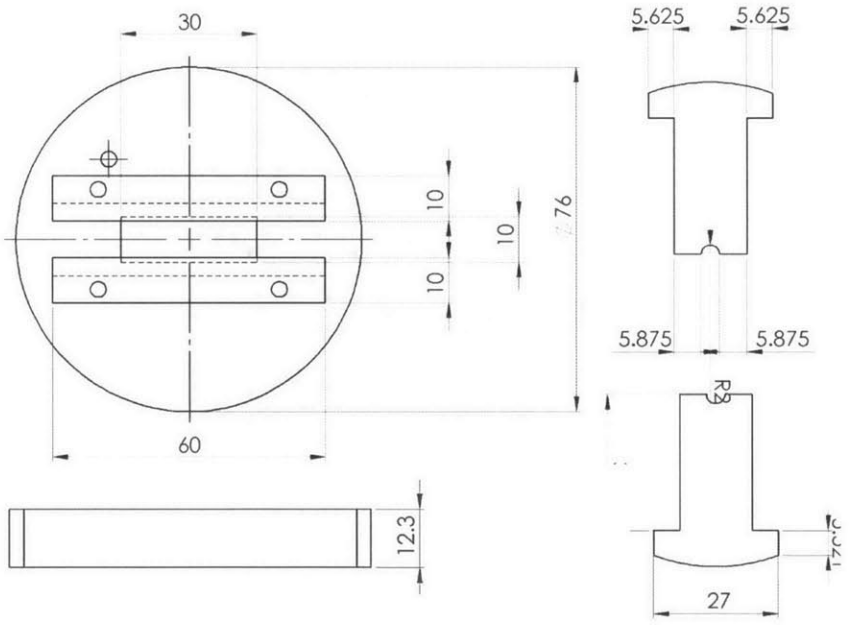

Figure 3-12: Technical drawing of the lid

3.3.2 Condensation on the Lid

Once the lid was in place, the next experimental difficulty faced was that of condensation of water vapor on the lid. This problem was overcome by heating the lid using

a strip heater controlled by a separate Proportional-Integral-Derivative (PID) controller. A thermocouple attached to the lid provided an input to the PID controller for controlling the heating of the lid such that the lid maintained a preset temperature. The thermocouple was calibrated in a separate water bath with the help of the Teflon thermistor probe. To prevent condensation and reduce thermal gradients, the temperature of the lid was set within 1-4 °C of the solution temperature.The solution temperature was intentionally not exceeded as the PID controlled strip heater was found to affect the stability of the temperature of the test solution for set temperatures greater than the solution temperature. This was because the temperature controller in the recirculator had a much finer control bandwidth (0.03°C) in comparison with PID controller for the lid heater (0.1°C). To further help reduce temperature fluctuations, insulation was also used around the lid. The complete assembly of the lid, heater, Wilhelmy plate and insulation is shown in Fig. 3-13.

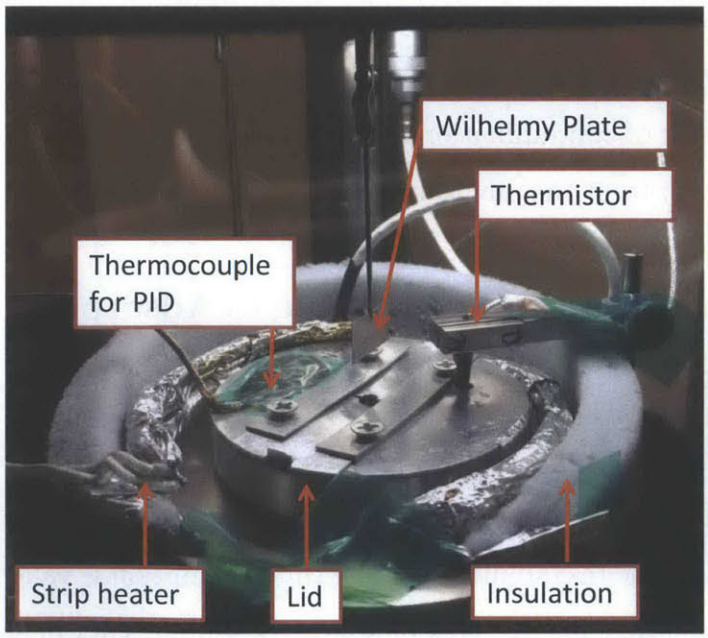

Figure 3-13: Photograph of lid with heater and insulation

3.3.3 Condensation on the Wilhelmy plate

The problem of condensation on the Wilhelmy plate and the solution to the problem was discussed in Section 3.1.1 and in Fig. 3-4. Surface tension was observed to rise with time due to condensation on the plate and attachment rod after taring of the balance and during measurement. This was minimized by reducing the duration of recording of surface tension.

3.3.4 Contamination

Contamination was another problem faced during experimentation. The slightest trace of organic contaminants was found to affect surface tension drastically. To prevent contamination, strict cleaning protocols and handling protocols were followed. During the handling of solutions, care was taken to ensure that the solutions in beakers and bottles were exposed to the environment only for a small duration of time. Gloves were worn during handling of the beakers, bottles and solutions. The cleaning protocols that were followed are talked about in more detail in Section 3.4. Apart from cleaning and handling protocols, the presence of a lid significantly contributed to reducing the risk of contamination as the lid restricted organic vapor diffusion and dust contamination from the environment into the test solution sample.

3.3.5 Contact Angle Changes due to Adsorption on Platinum Plate

One of the central assumptions used in the measurement of surface tension using a platinum Wilhelmy plate is the assumption of a zero contact angle between the platinum plate and the test solution. While this assumption is valid generally, a point of concern was whether precipitates of sparingly soluble salts in seawater adsorbing onto the platinum plate could result in the formation of a contact angle between the plate and the seawater test solution sample. To verify that seawater solutions had zero contact angles with the platinum plate even in the presence of precipitates at high temperatures and salinities, contact angle measurements of seawater solutions

on the platinum plate were conducted using a goniometer. The cases tested out are summarized in Table 3.3:

Table 3.3: Summary of contact angles tests

Case	Test solution	Temperature	Precipitates	Plate
1	Deionized water	23°C	No	Unscaled
2	75g/kg ASTM seawater	50°C	Yes	Unscaled
3	75 g/kg ASTM seawater	90°C	Yes	Unscaled
4	35 g/kg ASTM seawater	90°C	Yes	Unscaled
5	35 g/kg ASTM seawater	90°C	Yes	Scaled

As a control case, deionized water at room temperature was dropped onto the platinum Wilhelmy plate and the contact angle was measured using the goniometer. As expected, the deionized water completely wetted the plate resulting in a zero contact angle. Subsequently, measurements were conducted on ASTM seawater of approximate salinity $S = 75$ g/kg near 50°C and near 90°C to test whether precipitates of inverse solubility salts could cause a non-zero contact angle between the platinum plate and seawater test solution. Tests were conducted at 50°C and 90°C to see whether precipitates at higher temperatures affected the contact angle. A zero contact angle was observed for both cases.

To further establish that there was a zero contact angle with the platinum plate, a final experiment was conducted using a scaled Wilhelmy plate. ASTM seawater of salinity $S = 35$ g/kg was dropped onto the plate and allowed to fully evaporate and form a fine layer of scale on the platinum plate. A new test was conducted on this plate. The contact angle was again observed to be zero. This is depicted in Fig. 3-14. It was thus conclusively established that scaling and precipitation did not result in a contact angle between the test solution and the Wilhelmy plate.

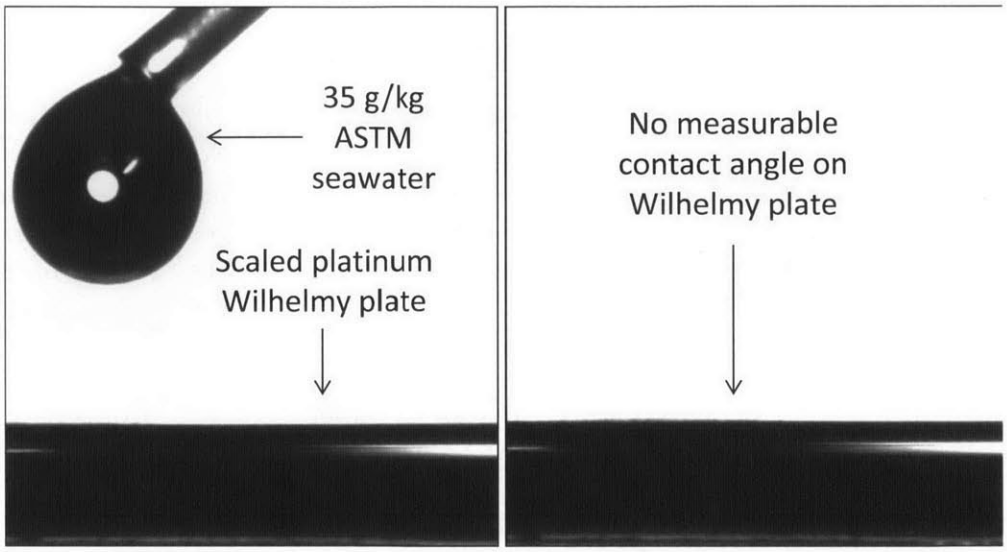

Figure 3-14: Contact angle measurement of 35 g/kg ASTM seawater on a platinum Wilhlemy plate scaled by sea salt

3.4 Cleaning Protocol

Glassware used for test solution preparation and the test beaker used to hold the test solution sample were cleaned by rinsing three times with Milli-Q deionized water [56]. The test beaker was rinsed additionally with ACS reagent grade water. Rinsed glassware was dried in an oven before use. Ultra clean task wipes [57] were used to absorb any left over water droplets. To reduce contamination risks new glassware was used whenever a fresh batch of test solution was prepared. The above mentioned cleaning procedure was found to be effective for experiments conducted on ACS water and aqueous sodium chloride. However, the procedure was not effective at removing scales that formed on the test beaker after extended testing of seawater at elevated temperatures ($T > 50°C$). Thus new test beakers were used for experiments carried out on seawater. A brief discussion regarding the effect of scale formation on surface tension measurement is discussed in Section 4.6.

Gloves were used at all times during preparation and testing. Care was taken

to ensure that the test solutions were exposed minimally to the environment. The lid was kept on the test beaker at all times to prevent particulate contamination from the environment. Once a test solution sample was poured into the test beaker, nothing was inserted into the test solution sample. The thermistor probe was rinsed and cleaned with Milli-Q deionized water before and after each set of experiments to prevent contamination. The Teflon construction further aided in preventing contamination. The lid was also rinsed and cleaned with Milli-Q deionized water after each set of experiments.

The Wilhelmy plate was rinsed with Milli-Q deionized water and flame cleaned after each surface tension measurement. This is depicted in Fig. 3-15.

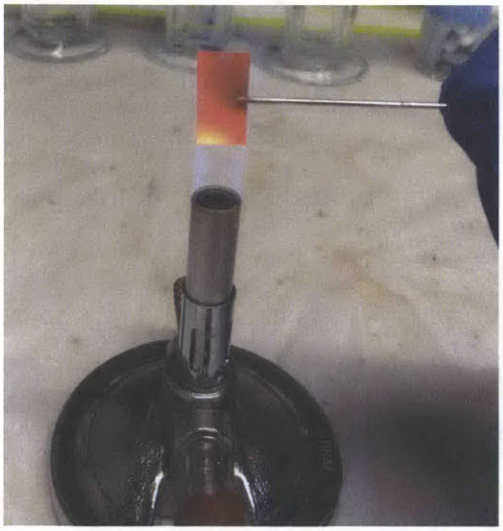

Figure 3-15: Flame cleaning of the Wilhelmy plate

3.5 General Procedure

The testing process began with first cleaning the test beaker according to the procedure laid down in Section 3.4. Once the test beaker was clean and dry, a stir bar and a test solution sample of a known salinity is added to the beaker. The initial mass of test solution sample was measured using either Mass Balance A or Mass Balance C and the initial salinity (S_{initial}) was recorded.

After obtaining the initial weight, the test beaker assembly was placed in the tensiometer with the thermistor inserted. The test solution sample was then brought to the desired test temperature with the help of the circulator. Approximately one hour was required to achieve a steady state at each temperature. Subsequently, the Wilhelmy plate was rinsed with deionized water and flame cleaned and inserted through the lid into the moist air environment. The test solution sample was then stirred for 30 seconds to diffuse any thermal gradients that formed due to air influx from the environment when the plate was inserted through the lid.

After stirring, the solution was allowed to settle down for 3-4 minutes after which surface tension ($\gamma_i \pm \sigma_{\gamma_i}$) and static temperature (T_{s_i}) was measured. Immediately after measuring surface tension, the solution was stirred to obtain the bulk solution temperature (T_{b_i}). Surface tension and temperature measurements at the test temperature were repeated in the above manner until surface tension measurements approximately saturated. This typically took around one hour and involved taking at least 5 measurements. This is discussed in more detail in Section 3.6.

The test solution sample was then heated 10°C to the next test temperature and a new set of surface tension measurements were conducted. Testing in this manner continued until 3 to 4 test temperatures were covered. At the end of testing the final mass of the test solution sample was measured using either Mass Balance A or Mass Balance C and the final salinity (S_{final}) was calculated. The difference between initial and final salinities arose due to loss of solvent due to evaporation which occurred despite the presence of the lid. The exact salinity at each test point was then calculated by distributing the loss of vapor in a weighted manner - the method for which is described in Section 3.6.3.

3.6 Data Analysis

To reduce the uncertainty in measurements, average values of surface tension ($\overline{\gamma}$), bulk solution temperature ($\overline{T_b}$) and salinity ($\overline{S}$) needs to be obtained. This section first describes a systematic trend observed in surface tension measurements and how

erroneous measurements of surface tension were excluded.

3.6.1 Surface Tension

As mentioned in Section 3.5, surface tension measurements at each test temperature was repeated at least five times. This led to the observation of a systematic trend in the measurements with the number of measurements, where surface tension measurements (γ_i) was observed to rise and eventually saturate. This was seen at every temperature and salinity point with the effect being more significant at elevated temperatures and when the test solution sample had contaminants. This was thought to be occurring because of the electronic compensation system in the microbalance. Regardless of the exact cause, this systematic trend was observed in all measurements.

To ascertain that the saturated values of surface tension were correct measurements, measurements of pure water at 20°C and at 80°C were compared with IAPWS correlation for the surface tension of pure water obtained from Eq. 2.11. This is depicted in Fig. 3-16. The line represents surface tension calculated from the correlation while the band represents the uncertainty of the correlation. The variation in surface tension arising from minor differences in temperature between measurements is also accounted for by the line. It can be clearly seen that measurements saturate to the actual values for surface tension.

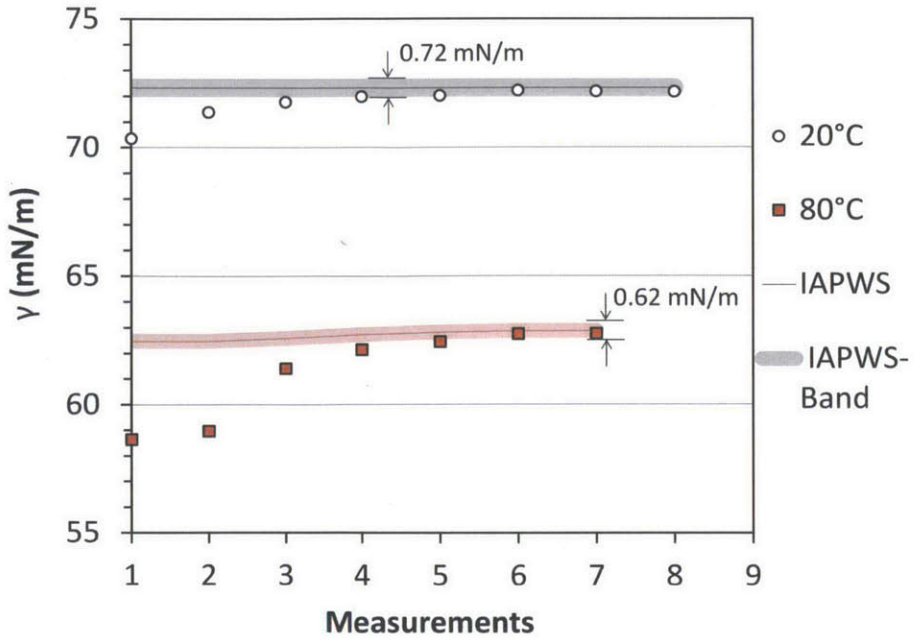

Figure 3-16: Plot showing surface tension measurements of ACS water at 20°C and 80°C saturating to expected values. The variation is presumed to be because of the electronic compensation mechanism in the microbalance

To systematically exclude measurements that are far from the saturated value and to include measurements close to the saturated value but not within the last five measurements, the Chauvenet's criterion described by Holman and Gajda [58] was modified and used. The procedure is described below:

1. Let the total number of measurements at a test temperature be 'N'.

2. The average ($\bar{\gamma}$) and the sample standard deviation ($s_{\bar{\gamma}}$) of the last 5 measurements is calculated.

$$\overline{\gamma} = \sum_{i=N-4}^{N} \gamma_i \tag{3.2}$$

$$s_{\overline{\gamma}} = \sqrt{\frac{1}{4} \sum_{i=N-4}^{N} (\gamma_i - \overline{\gamma})^2} \tag{3.3}$$

3. Next the deviation (d) of each of the N measurements with the average ($\overline{\gamma}$) is obtained

$$d_i = \gamma_i - \overline{\gamma} \tag{3.4}$$

4. The ratio $\frac{d_i}{\sigma_{\overline{\gamma}}}$ is then computed for each of the N measurements

5. If $\frac{d_i}{\sigma_{\overline{\gamma}}}$ is greater than 1.65 the measurement is excluded from the final data set while measurements within 1.65 are included.

   The number 1.65 here comes from the original Chauvenet's criterion which prescribes that for a normal distribution of 'k' points, an outlier is defined as a point whose probability of occurrence is less than 1/2k. For 5 points, thus an outlier is a point whose probability of occurrence is less than 0.1. In terms of deviations this translates as 1.65 times the standard deviation from the mean.

6. A new average value for surface tension ($\overline{\gamma}$) and the sample standard deviation for the final set of 'n' measurements ($s_{\overline{\gamma}}$) is then calculated.

This procedure was applied to surface tension measurements described in Fig. 3-16 mentioned earlier to yield a final dataset depicted in Fig. 3-17.

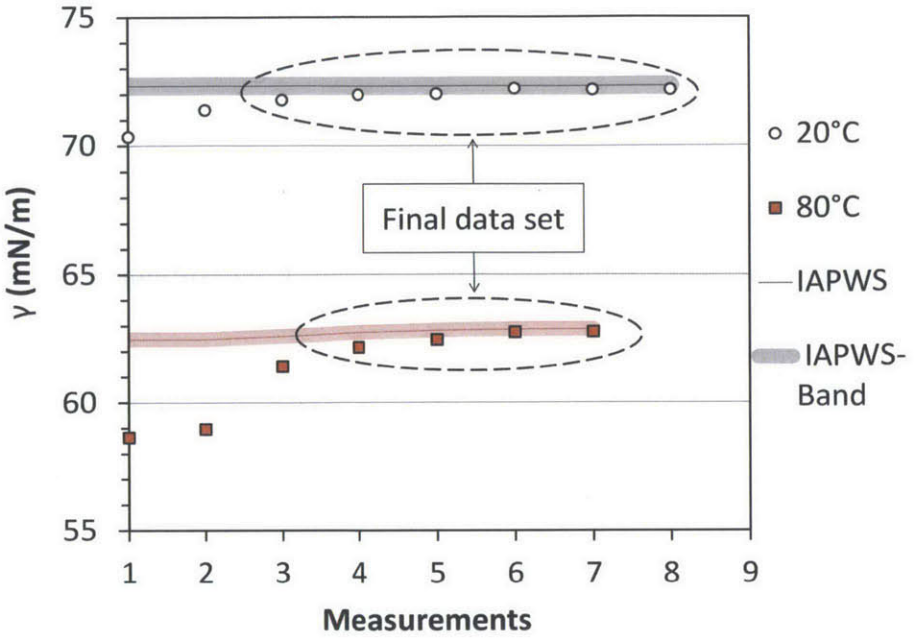

Figure 3-17: Plot showing surface tension measurements of ACS water at 20°C and 80°C after exclusion of measurements far from the saturated value

3.6.2 Temperature

The bulk solution temperatures (T_{b_i}) corresponding to the final set of surface tension measurements was used to calculate the average bulk solution temperature ($\overline{T_b}$) and the sample standard deviation in bulk solution temperature measurements ($s_{\overline{T_b}}$).

3.6.3 Salinity

As mentioned in Section 3.5, salinity was not measured at each test temperature but before and after an interval of 3 to 4 test temperatures. The initial salinity (S_{initial}) is known from test solution preparation and the final salinity (S_{final}) of the test solution sample is obtained by measuring the total mass of solvent lost ($m_{\text{solv,loss,total}}$). The loss in solvent mass resulted from evaporative losses that occurred despite the presence of the lid. The salinity (S_i) corresponding to each surface tension measurement was then calculated by distributing the total mass of solvent lost to evaporation across all surface tension measurements using a weighted average of the vapor pressure differ-

ence between the test solution sample and the environment. The model is described below:

1. The rate of loss of solvent due to evaporation at any instant is approximately proportional to the difference in vapor pressure of water vapor above the test solution surface ($P_{\text{vap,surf}}$) and vapor pressure of water vapor in the environment ($P_{\text{vap,env}}$).

$$\frac{\mathrm{d}m_{\text{solv,loss}}}{\mathrm{d}t} = B(P_{\text{vap,surf}} - P_{\text{vap,env}}) \tag{3.5}$$

The constant of proportionality (B) here is a function of the geometry of the lid and the test procedures and conditions, and is approximated as a constant within any one set of measurements. The vapor pressure above the test solution surface was approximated by the saturation vapor pressure for pure water at the corresponding solution bulk temperature (T_{b_i}). The vapor pressure of water vapor in the environment was calculated from psychrometry from the relative humidity (RH) and temperature in the environment which due to air-conditioning is approximately held constant at 24°C and 25% RH. This was measured using a digital hygrometer/thermometer manufactured by the Control Company. The instrument had a NIST traceable calibration.

2. The total mass of solvent lost, time duration (Δt_i) between surface tension measurements and the vapor pressure difference between the test solution sample and the environment ($P_{\text{vap,diff},i}$) during each surface tension measurement is known and Eq. 3.5 can be discretely integrated across the complete set of surface tension measurements (N_{total}) to obtain a value for 'B'.

$$P_{\text{vap,diff,i}} = P_{\text{vap,surf},i} - P_{\text{vap,env},i} \tag{3.6}$$

$$m_{\text{solv,loss,total}} = B \sum_{i=1}^{N_{\text{total}}} P_{\text{vap,diff},i}\ \Delta t_i \tag{3.7}$$

$$B = \frac{m_{\text{solv,loss,total}}}{\sum_{i=1}^{N_{\text{total}}} P_{\text{vap,diff},i}\ \Delta t_i} \tag{3.8}$$

3. From the obtained value of 'B', the mass of solvent lost ($\Delta m_{\text{solv,loss},i}$) during each surface tension measurement was calculated.

$$\Delta m_{\text{solv,loss},i} = B\ P_{\text{vap,diff},i}\ \Delta t_i \tag{3.9}$$

4. The mass of the test solution sample ($m_{\text{soln},i}$) during each surface tension measurement was then obtained from the known initial mass of the solution ($m_{\text{soln,initial}}$) and the salinity (S_i) corresponding to each surface tension measurement was then calculated. It must be noted here that S_1 corresponds to S_{initial} and S_n corresponds to S_{final}.

$$m_{\text{soln},i} = m_{\text{soln,initial}} - \sum_{k=1}^{i} \Delta m_{\text{solv,loss},k} \tag{3.10}$$

$$S_i = S_{\text{initial}} \frac{m_{\text{soln,initial}}}{m_{\text{soln},i}} \tag{3.11}$$

5. The salinities (S_i) corresponding to the final set of surface tension measurements was then averaged to obtain an average salinity ($\overline{S}$) and the sample standard deviation in salinity ($s_{\overline{S}}$).

The model was validated by measuring intermediate values of salinity ($S_{\text{meas},i}$) during 3 experiments conducted on ASTM seawater and comparing these with values of salinity calculated using the model (S_i). The comparison along with the initial salinity, final salinity, time period of measurement and the test temperature is shown in Table 3.4. The root mean square deviation between calculated and measured salinities was 0.06 g/kg while the maximum deviation was 0.09 g/kg. The maximum deviation of 0.09 g/kg was taken to be the uncertainty in salinity contributed by the model.

Table 3.4: Comparison of calculated and measured salinities for experiments conducted on ASTM seawater with the deviations for intermediate salinity measurements depicted in bold

Sl. No.	S_{initial} (g/kg)	S_{final} (g/kg)	t_i (hr)	T (°C)	S_i (g/kg)	$S_{\text{meas},i}$ (g/kg)	$S_i - S_{\text{meas},i}$ (g/kg)
1	20.01	21.29	0.0	24	20.00	20.01	0.00
			1.1	71	20.31	20.27	**0.04**
			1.9	81	20.63	20.55	**0.09**
			2.9	91	21.29	21.29	0.00
2	79.39	79.86	0.0	24	79.39	79.39	0.00
			0.8	40	79.52		
			1.7	51	79.78	79.74	**0.04**
			5.7	10	79.82		
			6.5	20	79.86	79.86	0.00
3	121.54	126.74	0.0	24	121.54	121.54	0.00
			1.7	2	121.54		
			2.8	10	121.56		
			3.8	30	121.67	121.73	**-0.06**
			4.6	40	121.85		
			5.7	52	122.28	122.31	**-0.03**
			6.8	61	122.97		
			7.8	71	124.12	124.20	**-0.08**
			9.4	81	126.74	126.74	0.00

3.7 Uncertainty Analysis

Uncertainty analysis was performed on the final data set of measurements obtained after the data refinement procedure outlined in Section 3.6. The methodology of uncertainty analysis was adopted was adopted from guidelines recommended by the Bureau of International Weights and Measurements [59] as well as books written by Patience [60] and Beckwith et al. [23].

3.7.1 Surface Tension

Since surface tension was measured directly, the contribution to uncertainty in surface tension arising from temperature and salinity variation is already captured by the measurements of surface tension. Thus, there are only two contributions to uncertainty of an average surface tension measurements for a particular test temperature and salinity:

1. Uncertainty in each surface tension measurement ($\sigma_{\gamma i}$)
2. Standard error of the sample of surface tension measurements at a particular temperature and salinity ($se_{\overline{\gamma}}$)

As mentioned in Section 3.1.1, the uncertainty in each surface tension measurement is known at the time of each measurement of surface tension.

The standard error of the sample is obtained from the sample standard deviation:

$$s_{\overline{\gamma}} = \sqrt{\frac{1}{n-1}\sum_{i=1}^{n}(\gamma_i - \overline{\gamma})^2} \tag{3.12}$$

$$se_{\overline{\gamma}} = \frac{s_{\overline{\gamma}}}{\sqrt{n}} \tag{3.13}$$

A combined uncertainty for each surface tension measurement is then obtained by taking a root mean square sum of the both uncertainty contributions:

$$u_{c\overline{\gamma}} = \sqrt{se_{\overline{\gamma}}^2 + \frac{\sum_{i=1}^{n}{\sigma_{\gamma i}}^2}{n}} \tag{3.14}$$

The expanded uncertainty is then obtained by multiplying the combined uncertainty ($u_{c\overline{\gamma}}$) with a coverage factor 'k', obtained from the t-value for the desired confidence interval (α) and number of final measurements (n).

$$U_{\overline{\gamma}} = k u_{c\overline{\gamma}} \tag{3.15}$$

$$k = t(1 - \alpha, n - 1) \tag{3.16}$$

A 95% confidence interval was used for calculating the expanded uncertainty. For m = 5, this resulted in a 'k' value of 2.777.

3.7.2 Temperature

The expanded uncertainty in the average bulk temperature ($U_{\overline{T_b}}$) is obtained using an approach similar to that of surface tension Most of the uncertainty was caused by temperature fluctuations in the test solution due to heat loss to the environment during surface tension measurements. A 95% confidence interval resulted in an average uncertainty of 0.11°C and a maximum uncertainty of 0.54°C. The maximum uncertainty occurred during the testing of aqueous sodium chloride at $T \approx 87.92$°C and $S = 123.41$ g/kg.

The results and correlations discussed in Chapter 4 use the bulk average temperatures. Static temperature measurements were taken to estimate the thermal gradient within the test solution sample. The difference between static and bulk temperatures varied from 0.05 to 0.5°C. However this did not contribute to the uncertainty in measuring the average bulk temperature.

3.7.3 Salinity

There are 5 sources of uncertainty that contribute to the combined uncertainty in average salinity ($u_{c\overline{S}}$). These are:

1. Uncertainty in salinity of the original solution ($u_{\overline{S},\text{orig}}$):

This was 0.01 g/kg for aqueous sodium chloride, 0.02 g/kg for ASTM seawater and 0.07 g/kg for ASCS seawater.

2. Uncertainty in salinity arising from test solution preparation ($u_{\overline{S},\text{prep}}$):

   This was 0.01 g/kg for all test solutions except for ASTM seawater of salinity $S = 121.54$ g/kg where the uncertainty in preparation was 0.05 g/kg.

3. Uncertainty in salinity arising from mass measurements of the test solution sample ($u_{\overline{S},\text{test}}$):

   The accuracy of the mass balance (0.01 g) used for weighing the test solution sample contributed to an uncertainty in salinity of 0.01 g/kg.

4. Uncertainty in salinity due to evaporation of the test solution sample during surface tension measurements ($u_{\overline{S},\text{evap}}$):

   The model described in Section 3.6.3 allowed the calculation of salinities corresponding to the 'n' final surface tension measurements. The standard error ($se_{\overline{S}}$) in salinity was then calculated from the sample standard deviation in salinity ($s_{\overline{S}}$). A 95% confidence interval was subsequently used to obtain the uncertainty arising from evaporation.

$$se_{\overline{S}} = \frac{s_{\overline{S}}}{\sqrt{n}} \tag{3.17}$$

$$u_{\overline{S},\text{evap}} = t(0.05, n-1)se_{\overline{S}} \tag{3.18}$$

5. Uncertainty in salinity arising from the model ($u_{\overline{S},\text{model}}$):

   As mentioned in Section 3.6.3, the maximum deviation of 0.09 g/kg between measured and calculated salinities was used as a conservative estimate of the uncertainty in salinity arising from the model.

The root mean square of individual contributions yielded the combined uncertainty in average salinity:

$$u_{c\overline{S}} = \sqrt{{u_{\overline{S},\text{orig}}}^2 + {u_{\overline{S},\text{prep}}}^2 + {u_{\overline{S},\text{test}}}^2 + {u_{\overline{S},\text{evap}}}^2 + u^2_{\overline{S},\text{model}}} \tag{3.19}$$

An average uncertainty in salinity of 0.17 g/kg and a maximum uncertainty in salinity of 0.82 g/kg was obtained using this approach. The maximum uncertainty in salinity occurred during the testing of ASTM seawater at $T = 87.40°C$ and $S = 130.96$ g/kg.

Chapter 4

Results and Discussion

Surface tension experiments were carried out on test solutions of ACS reagent grade water, aqueous sodium chloride solution, ASTM seawater and ASCS seawater at atmospheric pressure, across a temperature range of T = 0 - 90°C and salinity range of S = 0 - 120 g/kg. Temperature was varied in intervals of 10°C while salinity was generally varied in intervals of 40 g/kg. At each temperature and salinity point, at least five measurements of surface tension and bulk temperature were made. Subsequently, data analysis as described in Section 3.6 was conducted on the complete set of measurements to filter out erroneous measurements and for obtaining average values for surface tension, bulk temperature and salinity. The results presented in this section are thus final averaged measurements.

4.1 Validation

To validate the accuracy of the experimental procedure described in Chapter 3, surface tension experiments were conducted on ACS water and aqueous sodium chloride solutions at atmospheric pressure for salinities S = (0, 39.99, 80.19, 120.01) g/kg across a temperature range of T = 0 - 90°C. The experimental results were then compared with correlations from literature. For ACS water, the results were compared with the IAPWS correlation for the surface tension of water given by Eq. 2.11 and for aqueous sodium chloride the results were compared with the correlation developed by

Dutcher et al. given by Eq. 2.4. The results of these are showed in Fig. 4-1.

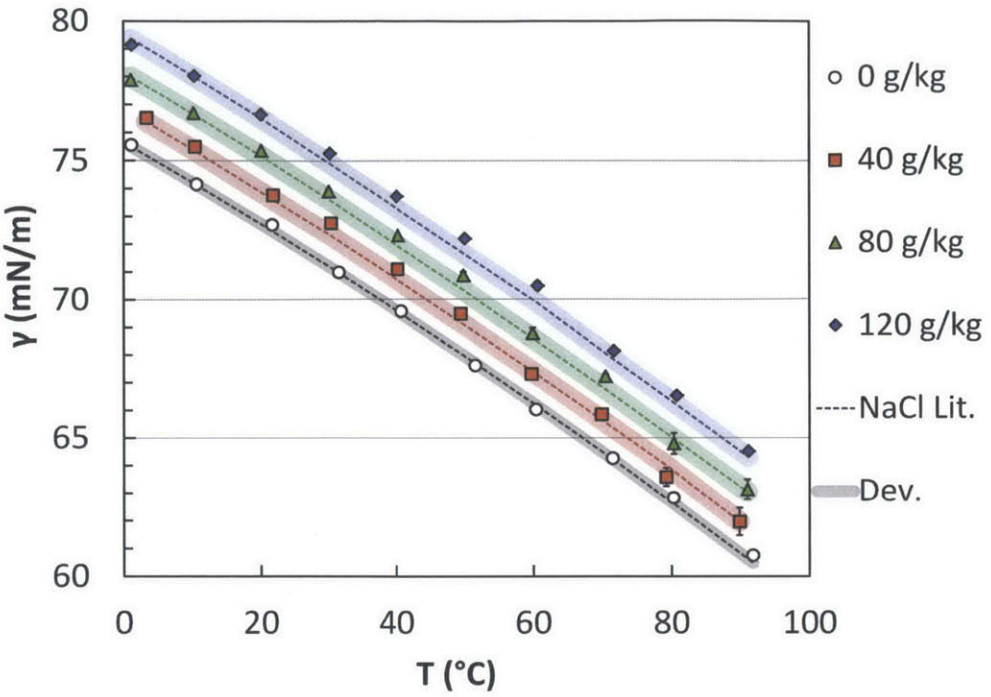

Figure 4-1: Comparison of present measurements of surface tension of pure water and aqueous sodium chloride solutions to values from literature correlations

The points represent average surface tension measurements obtained at each temperature and salinity. The vertical error bars represent the expanded uncertainty in the surface tension measurements. The uncertainty in temperature was too small to be depicted. Figure labels represent aqueous sodium chloride measurements in salinity intervals of 40 g/kg for simplifying the figure. The actual salinity of the test solution did drift from the initial values during measurement due to evaporation however this was captured by the model described in Section 3.6.3. The maximum drift observed was an increase in salinity of 6.08 g/kg for tests conducted at $T = (70,$ 80 and 90)°C for a test sample of initial salinity $S = 120.01$ g/kg. The straight lines represent surface tension calculated from the literature correlations for the temperatures and salinities corresponding to the points measured. The colored band across the lines represents the average absolute error between the measured and calculated values in Dutcher's correlation for aqueous sodium chloride. For pure water, the band

represents the actual uncertainty. The results showed that the measurements made were within the within the accepted uncertainties of the correlation except at high temperatures and salinities.

The expanded uncertainty in surface tension measurements for ACS water and aqueous sodium chloride is depicted in Fig. 4-2. The maximum observed uncertainty in surface tension measurements was 0.49 mN/m at $T = 89.80°C$ and $S = 41.37$ g/kg, while the average uncertainty across the whole test range was 0.12 mN/m. The average uncertainty was however much lower at 0.07 mN/m for $T \leq 50°C$ while it was 0.18 mN/m for $T > 50°C$.

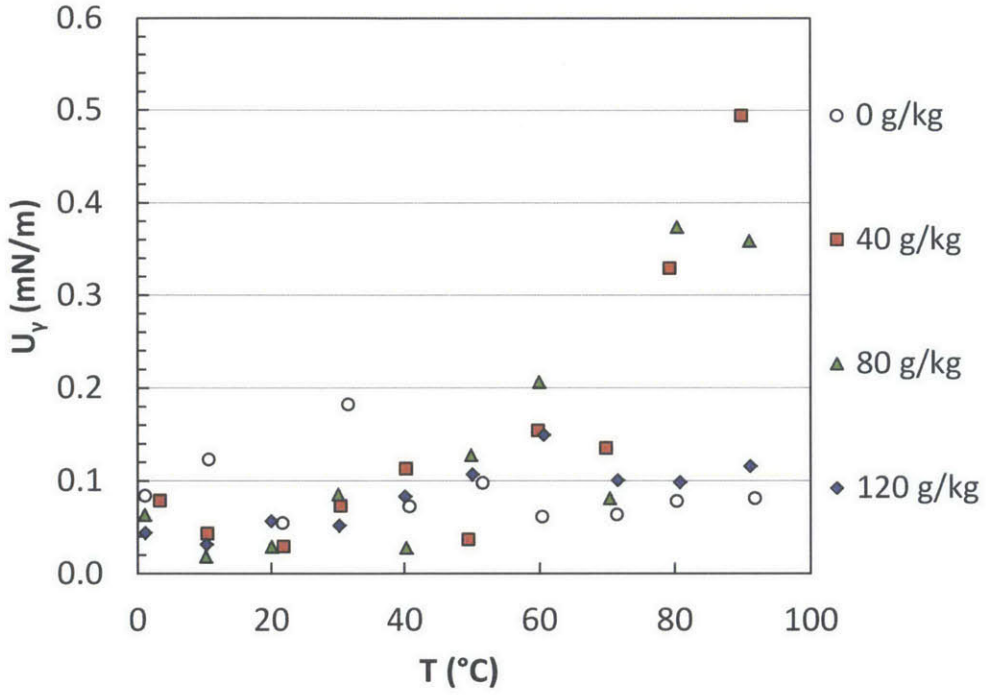

Figure 4-2: Expanded uncertainty in surface tension measurements for ACS water and aqueous sodium chloride solutions

The deviation between surface tension measurements and values calculated from the literature correlations is depicted in Fig. 4-3. The maximum deviation between surface tension measurements for ACS water and the corresponding IAPWS correlation values was 0.45% at $T = 91.75°C$. This was within the 0.5% uncertainty band of the IAPWS correlation. The maximum deviation between surface tension mea-

surements for aqueous sodium chloride and the correlation developed by Dutcher et al. was 0.89% at $T = 60.60°C$ and $S = 123.41$ g/kg. However, it must be noted here that Dutcher's correlation quoted only an average absolute error of 0.72%. To verify the actual error in Dutcher's correlation at salinities near 120 g/kg salinity, the results from Dutcher's correlation was compared to the high salinity raw data from Abramzon et al. [61] that Dutcher had used. The comparison showed a deviation of 1.71% for aqueous sodium chloride at $S = 100$ g/kg and $T = 60°C$. Thus a 0.89% deviation observed in this experiment still falls within the actual uncertainty of Dutcher's correlation.

The average absolute deviation between surface tension measurements and the literature correlations was 0.33%. For $T \leq 50°C$, the average absolute deviation was 0.31% while for $T > 50°C$, the average absolute deviation was 0.36%.

From the above discussion, it can be concluded that the experimental procedure was both valid and accurate.

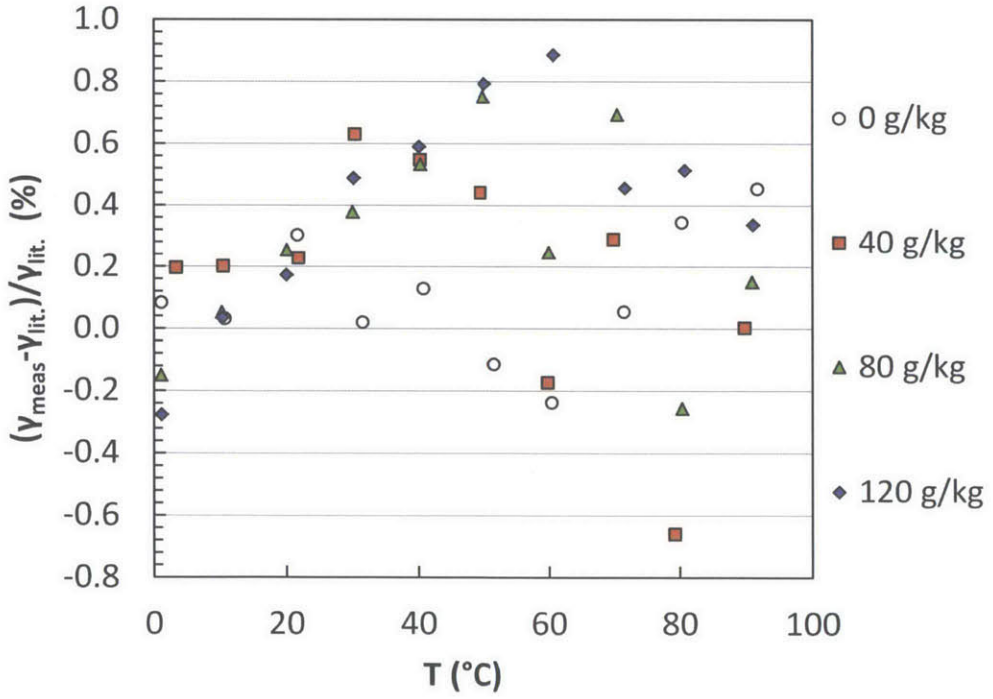

Figure 4-3: Deviation of surface tension measurements of ACS water and aqueous sodium chloride from the their corresponding literature correlations given by Eq. 2.11 and Eq. 2.4

4.2 Surface Tension of ASTM Seawater

The surface tension of ASTM seawater was characterized as a function of temperature and salinity at atmospheric pressure. Surface tension experiments were performed on on seawater of absolute salinities $S = (20.01, 35.18, 40.49, 79.39, 121.54)$ g/kg across a temperature range of 0 to 90°C in intervals of 10°C. The resulting set of 50 average measurements of surface tension, bulk temperature, and salinity is listed in Appendix A. The measurements are also plotted in Fig. 4-4.

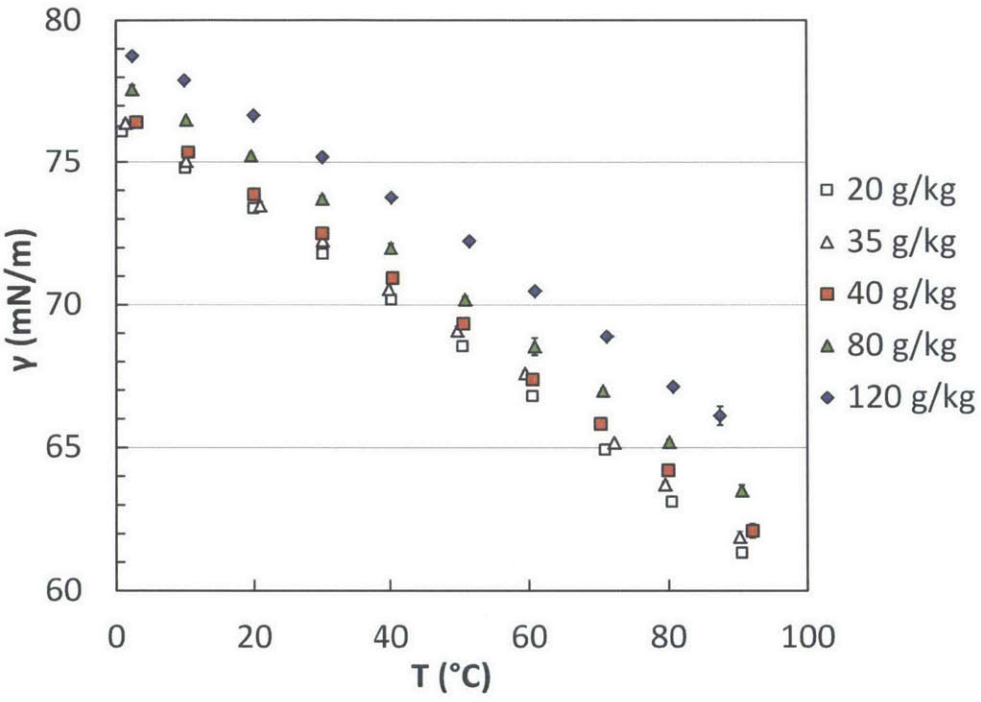

Figure 4-4: Complete set of measurements for surface tension of ASTM seawater

The uncertainty in the average surface tension measurements is depicted in Fig. 4-5. The maximum uncertainty was 0.33 mN/m at a $T = 87.40$°C and $S = 131.96$ g/kg while the minimum uncertainty was 0.04 mN/m at $T = 2.29$°C and $S = 121.54$ g/kg. The average uncertainty for all measurement was 0.12 mN/m. For $T \leq 50$°C, the average uncertainty was 0.11 mN/m while for $T > 50$°C, the average uncertainty was 0.15 mN/m.

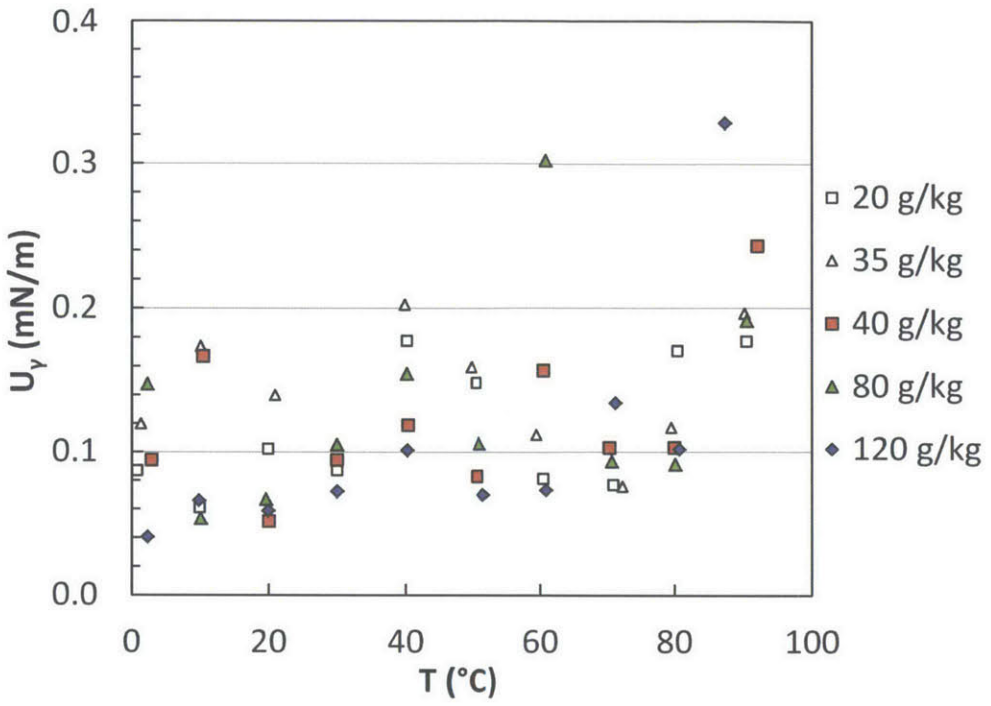

Figure 4-5: Expanded uncertainty in surface tension measurements for ASTM seawater

The final average measurements of surface tension, bulk temperature and salinity was fit to obtain the following best fit correlation:

$$\gamma_{sw} = \gamma_w \left[1 + 3.766 \times 10^{-4}\ S + 2.347 \times 10^{-6}\ S\ T\right] \tag{4.1}$$

where, γ_{sw} is surface tension of seawater in mN/m, γ_w is the surface tension of pure water in mN/m as calculated from the IAPWS correlation given by Eq. 2.11, S is absolute salinity in g/kg, and T is temperature in Celsius in the current ITS-90 temperature scale.

The fit had a coefficient of determination (R^2) value of was 0.999. The average absolute deviation of data from the fit was found to be 0.19% while the maximum deviation was +0.60% at $T = 51.48$°C and S = 122.20 g/kg. The deviation between measured and calculated values is depicted in Fig. 4-6.

The form of the fit was similar to that used by Chen et al. in Eq. 2.10 and is a simple function generally used to describe the variation of surface tension of

aqueous electrolytes at low salt concentrations [31] where the ions are solvated by water molecules rather than water molecules being solvated by ions.

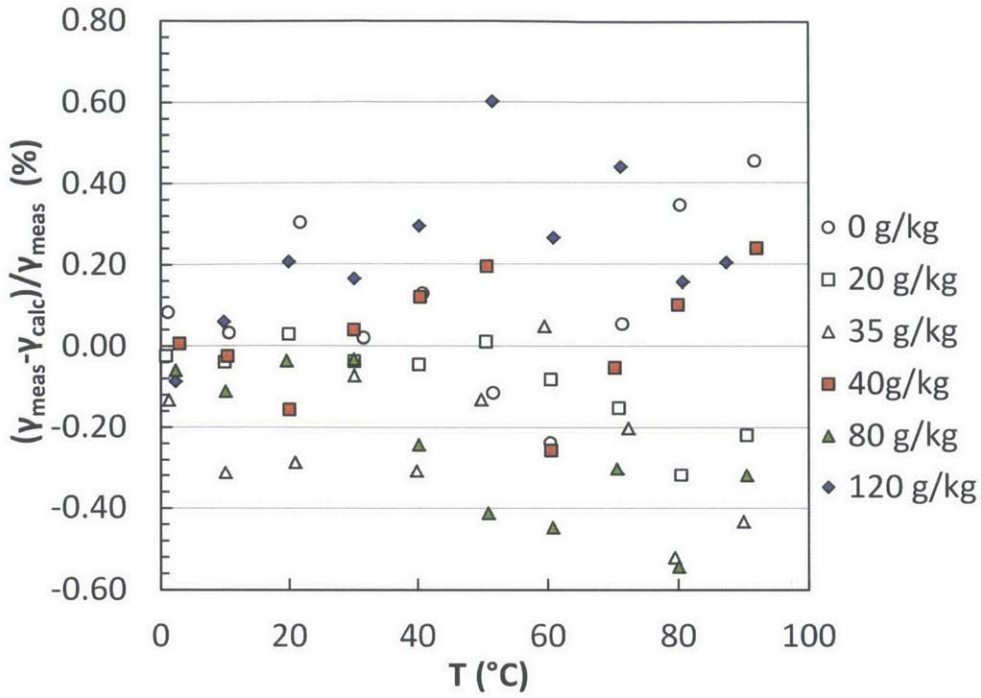

Figure 4-6: Deviation of surface tension measurements of ASTM seawater from surface tension calculated by Eq. 4.1

The correlation shown in Eq. 4.1 was compared with the most recent seawater surface tension data from Chen et al. [1] (S = 5 - 35 g/kg and T = 10 - 40°C) and the deviation between them was plotted in Fig. 4-7. The average absolute deviation between Eq. 4.1 and Chen's data was found to be 0.20% while the maximum deviation was -0.47% at T = 14.778°C and S = 34.486 g/kg. This was within the maximum deviation of 0.60% observed in the correlation developed in this work.

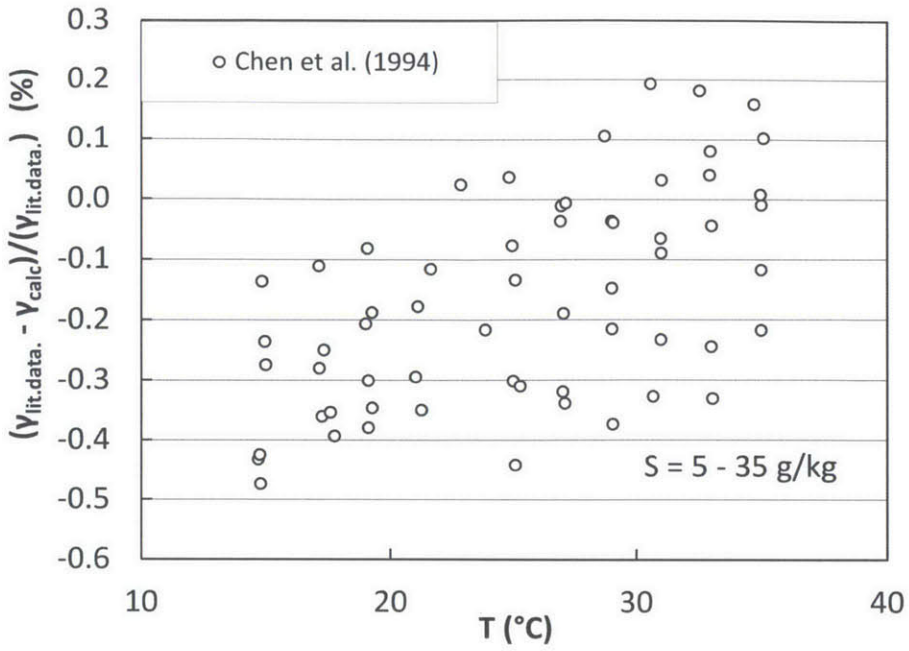

Figure 4-7: Deviation of seawater surface tension data of Chen et al. [1] from surface tension calculated using Eq. 4.1

4.3 Comparison of Surface Tension of ASTM Seawater with Aqueous Sodium Chloride

The surface tension measurements for ASTM seawater of salinities S = (20.01, 35.18, 40.49, 79.39, 121.54) g/kg was also compared with the correlation developed by Dutcher et al. for aqueous sodium chloride, given by Eq. 2.4. Figure 4-8 depicts this comparison for initial salinities S = (40.49, 79.39, 121.54) g/kg. The figure also depicts the IAPWS correlation for the surface tension of water, Eq. 2.11, for reference. The points depicted represent the average surface tension measurements carried out at each temperature and salinity. The lines represent surface tension calculated from the literature correlations for pure water and aqueous sodium chloride. The band corresponding to aqueous sodium chloride represents the average absolute deviation between the measured and calculated values in Dutcher's correlation for aqueous sodium chloride. For pure water, the band represents the actual uncertainty. The vertical error bars represent the expanded uncertainty in the surface tension measure-

ments. It can be seen from the results that the seawater surface tension measurements were within the error band of the correlation except at $T \geq 50$°C for ASTM seawater of salinity $S = 121.54$ g/kg.

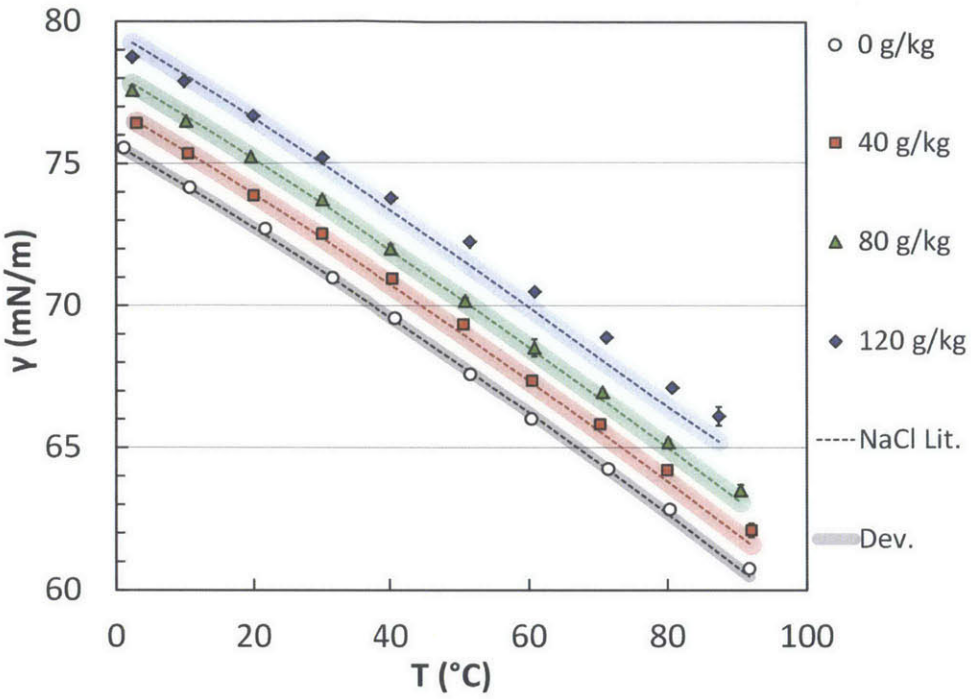

Figure 4-8: Surface tension of ASTM seawater compared with Dutcher's correlation for aqueous sodium chloride

The deviation of surface tension measurements for ASTM seawater from the surface tension of aqueous sodium chloride calculated using Dutcher's correlation is illustrated in Fig. 4-9. While measurements generally fit within the 0.72% average absolute error of Dutcher's correlation, the deviation was found to be higher at around 1.20% for ASTM seawater of initial salinity $S = 121.54$ g/kg at $T \geq 50$°C. The average absolute deviation was 0.33% while the maximum deviation was 1.37% at $T = 87.40$°C and $S = 130.96$ g/kg. From a practical point of view, since the maximum deviation was only 1.37%, the approximation of seawater surface tension by aqueous sodium chloride may still be considered to be valid within the thermal desalination operating range ($T = 40$ - 100°C and $S = 40$ - 120 g/kg). However, for greater accuracy especially at high salinities and high temperatures, it is recommended to use

the correlation developed in this work for seawater surface tension, given by Eq. 4.1.

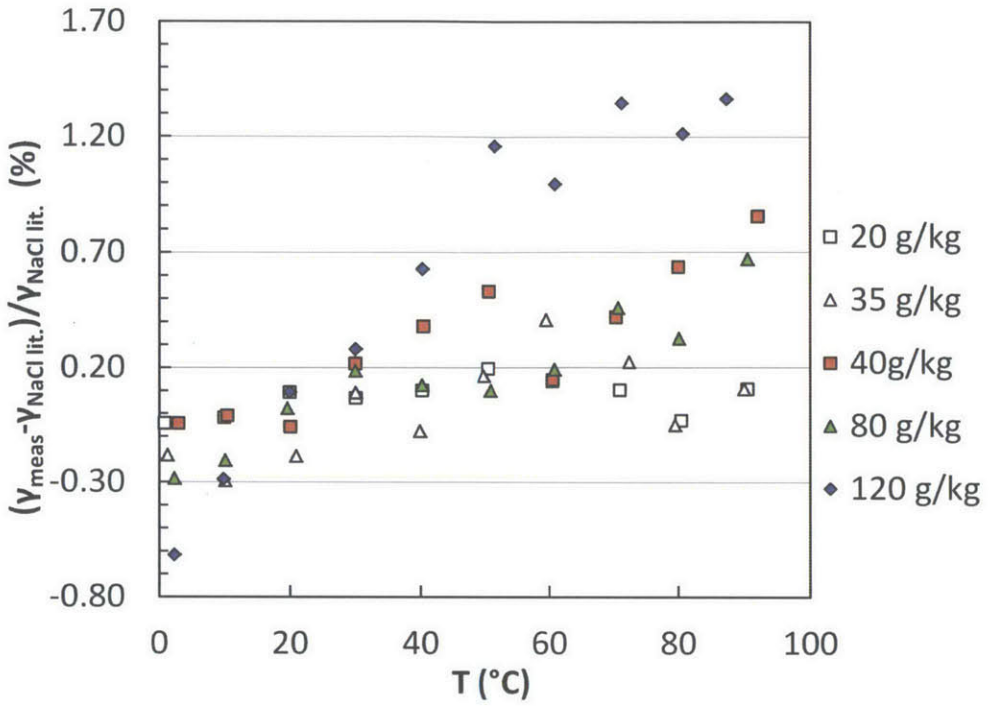

Figure 4-9: Deviation of surface tension measurements of ASTM seawater from surface tension of aqueous sodium chloride calculated using Dutcher's correlation, Eq. 2.4

4.4 Comparison of ASTM and ASCS Seawater

To ascertain whether the results obtained for ASTM seawater could be extended to properly treated natural seawater, experiments were conducted on ASCS seawater ($S = 35.16$ g/kg) across a temperature range of 0 to 90°C in intervals of 10°C. As mentioned in Section 3.2, seawater from the surface of the Atlantic ocean is microfiltered and treated with ultraviolet radiation by the commercial supplier to obtain ASCS seawater. The exact organic content of ASCS seawater is not known, but it is expected that there are still trace amounts of organic contaminants since the supplier has mentioned that ASCS seawater is not sterile and has a shelf life of only 12 months. Additionally ASCS seawater also contains several heavy metals not present in ASTM seawater.

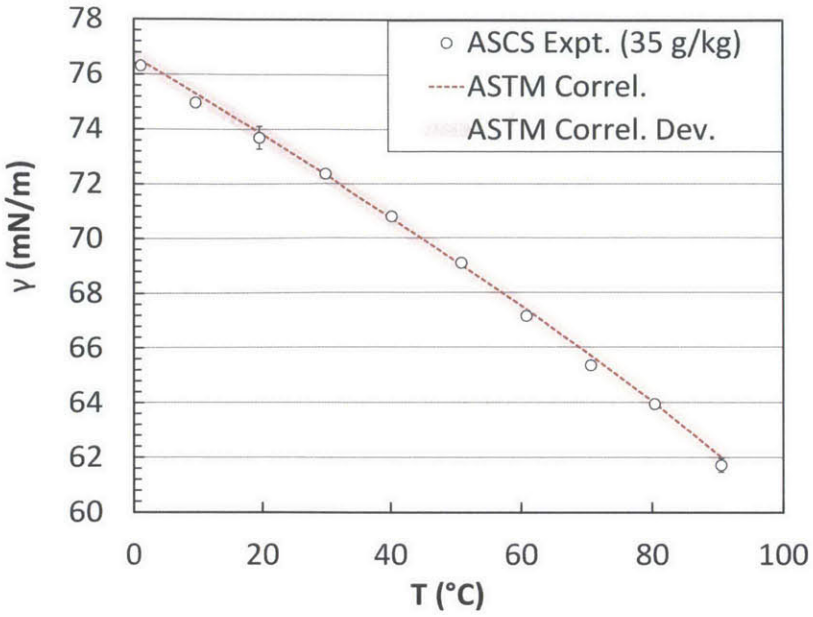

Figure 4-10: Surface tension measurements of 35.16 g/kg ASCS seawater compared with the results of the best fit correlation for ASTM seawater given in Eq. 4.1 along with a deviation band of 0.60%

Figure 4-10 depicts the results of these experiments. The points represent average surface tension measurements for ASCS seawater. The line represents the surface tension of ASTM seawater calculated from the correlation developed in Eq. 4.1. The band represents the maximum deviation of the correlation which was 0.60%. The vertical error bars represent the uncertainty in measurement. The maximum deviation between surface tension measurements for ASCS seawater and the best fit correlation for ASTM seawater was -0.53% at $T = 70.66°C$. This was within the uncertainty of the correlation. Thus the results for ASTM seawater can be extended to natural seawater, provided the natural seawater is treated properly. Trace organic content present in ASCS seawater after its treatment and the heavy metals present in ASCS seawater did not significantly affect its surface tension.

However, it must be noted that there can be a high degree of variation in the organic content in natural seawater across the world particularly near coastlines as well as inefficiencies in filtration and treatment. Thus, it is still possible for organic

surfactants to be still present post-treatment which could in turn lead to reduced surface tension. In practical engineering applications, the value for surface tension obtained from Eq. 4.1 can be used as an upper bound for the surface tension of natural seawater.

4.5 Precipitation of Sparingly Soluble Salts

During the experiments on seawater where the temperature of the test solution sample was heated to $T > 50°C$, precipitation of some of the constituent salts of seawater was observed. This was expected as beyond 50°C at seawater salinity, the solubility limits of sparingly soluble salts like calcium sulphate ($CaSO_4$), calcium carbonate ($CaCO_3$), magnesium carbonate ($MgCO_3$) and magnesium hydroxide ($Mg(OH)_2$) are reached [13]. The presence of these with the exception of magnesium hydroxide was qualitatively inferred by Energy Dispersive Spectrum (EDS) analysis of precipitates obtained from a sample of 35 g/kg ASCS seawater tested at $T = 80°C$. The results of the EDS analysis is depicted in Figure 4-11.

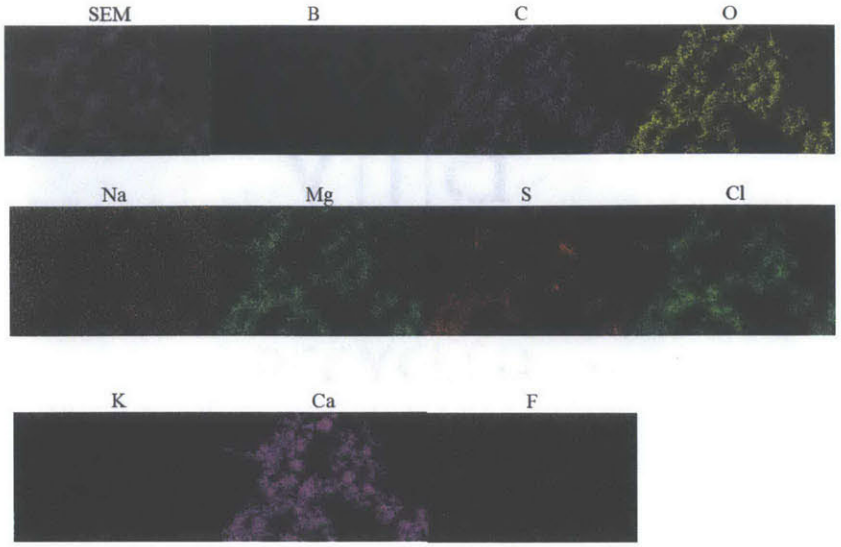

Figure 4-11: Results of Energy Dispersive Spectrum (EDS) analysis of a sample of precipitate obtained from 35 g/kg ASCS seawater tested at $T = 80°C$ showing the presence of elemental carbon, oxygen, magnesium, sulphur, chlorine and calcium along with an scanning electron microscope (SEM) image of the analyzed sample

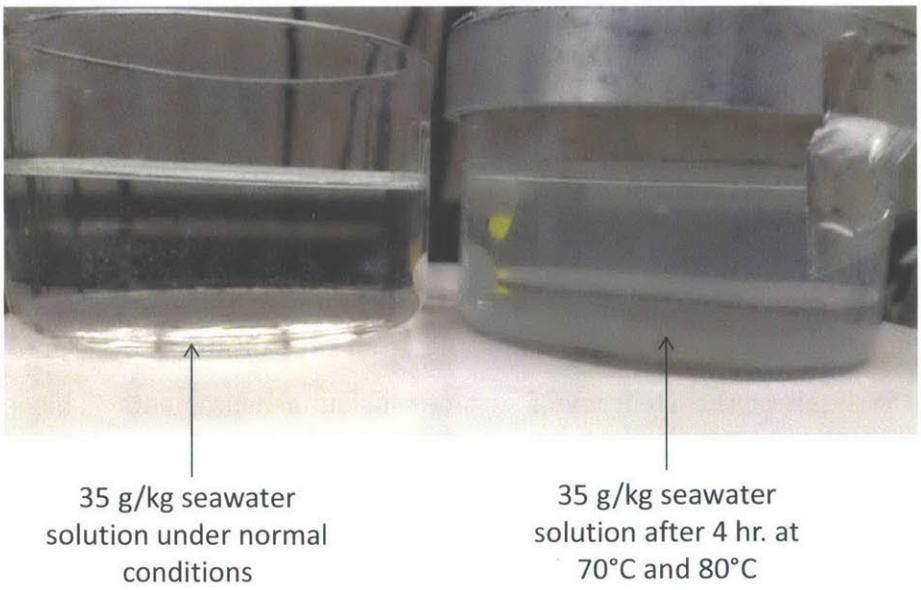

Figure 4-12: Comparison of 35 g/kg ASTM seawater under normal conditions and after 4 hours of testing at $T = 70°C$ and $80°C$

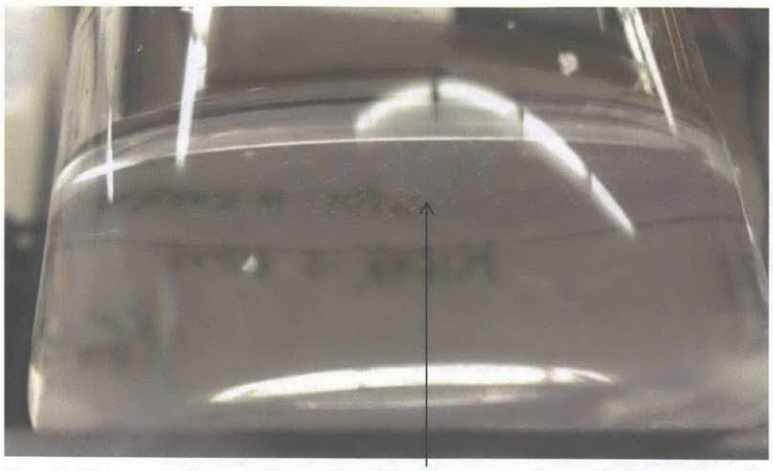

Figure 4-13: Precipitates the surface of 35 g/kg ASTM and after 4 hours of testing at $T = 70°C$ and 80°C

Precipitation was observed to cause turbidity in the bulk of test solution sample. This is illustrated in Fig. 4-12 where a 35 g/kg ASTM seawater sample under normal conditions is compared with a sample that underwent four hours of testing at $T = 70°C$ and 80°C. It was also observed that once precipitation occurred at $T > 50°C$, the seawater test solution sample did not return to its original clear state on cooling. Precipitates were also observed to be floating at the surface of the test solution sample as well. This is illustrated in Fig. 4-13. Despite this, precipitation was not found to affect the accuracy of surface tension measurements; in contrast permanent scale formation on the glass test beaker resulting from precipitation over time was found to significantly affect the accuracy of surface tension measurements. This is discussed in more detail in Section 4.6.

4.6 Effect of Scale Formation

While the precipitation of sparingly soluble salts in seawater test solution samples did not directly affect the accuracy of surface tension measurements significantly, "permanent" scale formation of the test beaker that occurred over a few hours of testing

at high temperatures ($T > 50°C$) was observed to affect surface tension measurements drastically.

This was observed in a controlled manner when surface tension measurements were carried out on a clean beaker over a period of 14 hours. Experiments were conducted in the following order,

1. 35.16 g/kg ASCS seawater from T = 60 - 90 °C in 10°C intervals
2. 79.39 g/kg ASTM seawater from T = 60 - 90 °C in 10°C intervals
3. 121.54 g/kg ASTM seawater from T = 60 - 90 °C in 10°C intervals
4. 40.49 g/kg ASTM seawater from T = 60 - 70 °C in 10°C intervals

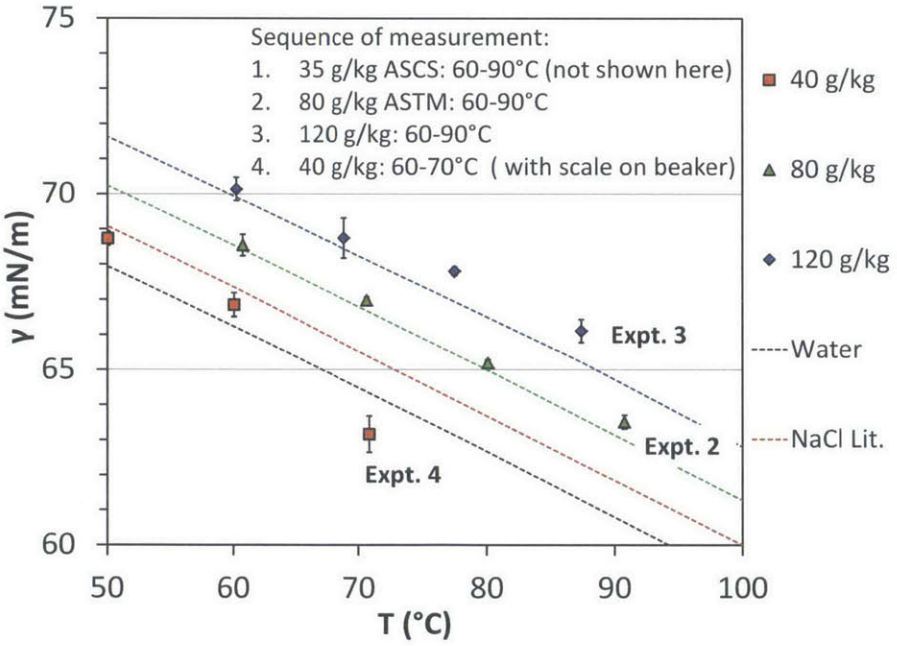

Figure 4-14: Surface tension decreasing below the surface tension of pure water after scale formation on the test beaker

The same test beaker was used for these experiments and between each experiment, the test beaker was cleaned according to protocols mentioned in Section 3.4. The results from these experiments are depicted in Fig. 4-14. While Experiments 1, 2 and 3 gave good results, the measured surface tension dropped from its expected

value in the 4th experiment on 40.49 g/kg ASTM seawater, decreasing even below the surface tension of pure water at $T = 70°C$.

The only parameter that changed in Experiment 4 from the earlier experiments was the formation of a fine "permanent" layer of scale on the test beaker. While Experiments 1 and 2 had led to precipitate residue or scale forming on the beaker, the cleaning procedure of rinsing with Milli-Q deionized water, ACS water and light scrubbing with task wipes was able to remove these. However, Experiment 3 conducted on 121.54 g/kg ASTM seawater resulted in scale formation on parts of the test beaker that could not could not be removed even after four rinses of Milli-Q deionized water and scrubbing with task wipes.

The depression of surface tension below that of pure water was further observed when surface tension experiments on ASTM seawater were conducted using the same test beaker over a longer period of time. These results are given in Fig. 4-15. The depression of surface tension was observed after $T > 50°C$ and was found to increase with increasing temperature and salinity.

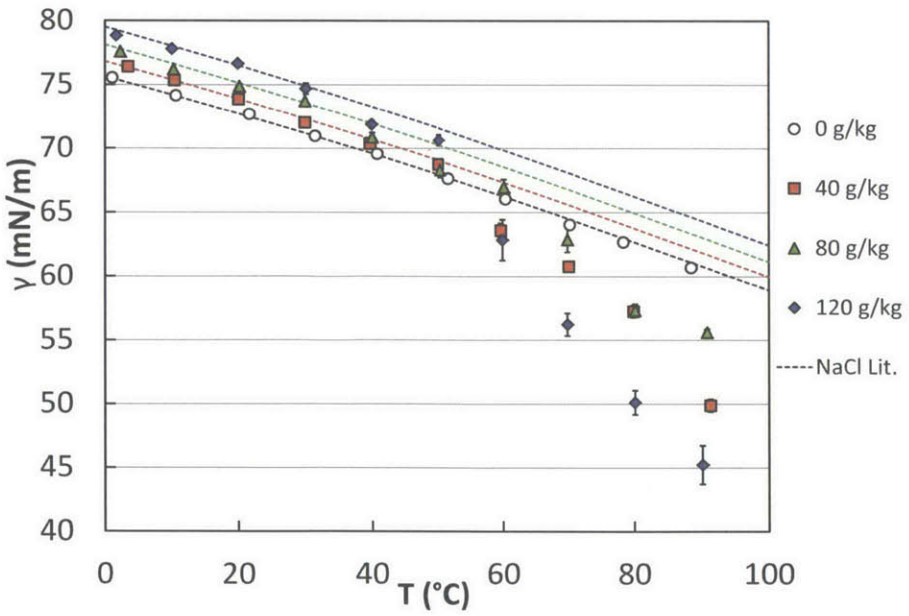

Figure 4-15: Surface tension decreasing below the surface tension of pure water after scale formation on the test beaker for $T > 50°C$

The exact reason for why surface tension decreased after scale formed and why the effect increased with salinity and temperature is not known. It is plausible that contaminants from the environment may have adhered to the layer of scale on the beaker. At temperatures less than $T = 50°C$, the scale layer may not have been actively interacting with the test solution sample hence contaminants did not affect the surface tension measured. However, at elevated temperatures, the scale on the beaker may have started diffusing into the solution carrying the contaminants with it which in turn reduced surface tension. However, this hypothesis was not tested.

What is clear is that scale formation led to higher uncertainty in surface tension measurements and also caused surface tension to decrease drastically at $T > 50°C$.

This observation may be relevant for real life applications such as membrane distillation and heat transfer in falling film evaporators in multi-effect distillation, scale does form and grow on membranes and heat transfer surfaces respectively. Thus, it is possible that with time, contaminants could accumulate on the scale and reduce surface tension of the seawater being concentrated thus affecting the process. This is primarily a concern for membrane distillation where the sensitivity of the process to surface tension is higher. It is thus recommended that further experiments be conducted to explore this aspect in greater detail.

Chapter 5

Conclusions

An accurate experimental procedure for determining the surface tension of electrolyte solutions at atmospheric pressure across a temperature range of T = 0 - 90°C was developed. The procedure was validated by conducting experiments on ACS reagent grade water and aqueous sodium chloride solutions.

Surface tension of ASTM seawater was measured accurately across a temperature range of T = 0 - 90°C and a salinity range of S = 0 - 120 g/kg. The uncertainty in measurements varied between 0.04 - 0.33 mN/m. The measurements were used to develop a best fit correlation for the surface tension of seawater as a function of temperature and salinity. The average absolute deviation of measurements from the correlation was 0.19% while the maximum deviation was 0.60%.

The surface tension of seawater was found to be comparable to within 1.37% of the surface tension of aqueous sodium chloride solutions of equivalent salinities.

Surface tension of ASTM D1141 standard seawater and ASCS seawater was found to be comparable suggesting that the organic content in 0.2 μm microfiltered and ultraviolet radiation treated natural open-ocean seawater is present in too trace an amount to affect surface tension.

Scale formation by sparingly soluble salts in seawater with time was observed to cause a reduction in surface tension. The exact mechanism is unknown and is an area for future work.

Appendix A

Experimental Data

The average measurements of salinity ($\overline{S}$), bulk temerature ($\overline{T_b}$), and surface tension ($\overline{\gamma}$) for ACS water, aqueous sodium chloride, ASTM seawater and ASCS seawater are listed here. The uncertainity in measurements, the number of points used for averaging 'n', and the coverage factor 'k' used for calculating uncertainty are also listed.

Table A.1: Measurements for ACS water

Sl. No.	$\overline{S}$ (g/kg)	$u_{c\overline{S}}$ (g/kg)	$\overline{T_b}$ °C	$U_{\overline{T_b}}$ °C	$\overline{\gamma}$ (mN/m)	$U_{\overline{\gamma}}$ (mN/m)	n	k
1	0.00	-	1.07	0.03	75.561	0.084	5	2.776
2	0.00	-	10.59	0.03	74.159	0.123	5	2.776
3	0.00	-	21.65	0.24	72.706	0.055	5	2.776
4	0.00	-	31.47	0.04	70.977	0.183	5	2.776
5	0.00	-	40.73	0.04	69.568	0.073	5	2.776
6	0.00	-	51.55	0.06	67.605	0.098	6	2.571
7	0.00	-	60.35	0.04	66.020	0.062	6	2.571
8	0.00	-	71.42	0.03	64.262	0.064	4	3.182
9	0.00	-	80.27	0.12	62.839	0.078	5	2.776
10	0.00	-	91.75	0.30	60.761	0.081	5	2.776

Table A.2: Measurements for aqueous sodium chloride

Sl. No.	$\overline{S}$ (g/kg)	$u_{c\overline{S}}$ (g/kg)	$\overline{T_b}$ °C	$U_{\overline{T_b}}$ °C	$\overline{\gamma}$ (mN/m)	$U_{\overline{\gamma}}$ (mN/m)	n	k
1	40.05	0.09	3.29	0.05	76.526	0.079	5	2.776
2	40.04	0.09	10.37	0.08	75.498	0.043	5	2.776
3	39.99	0.09	21.79	0.03	73.770	0.030	5	2.776
4	40.42	0.10	30.33	0.03	72.755	0.073	5	2.776
5	40.02	0.09	40.21	0.04	71.080	0.113	5	2.776
6	40.36	0.10	49.44	0.05	69.472	0.037	5	2.776
7	40.87	0.17	59.73	0.03	67.300	0.155	6	2.571
8	41.45	0.19	69.82	0.08	65.840	0.136	5	2.776
9	43.68	0.33	79.22	0.07	63.584	0.329	7	2.447
10	41.37	0.35	89.80	0.16	61.972	0.495	5	2.776
11	80.17	0.09	1.05	0.04	77.872	0.063	5	2.776
12	80.28	0.09	10.17	0.03	76.695	0.018	5	2.776
13	80.67	0.11	20.04	0.03	75.358	0.029	6	2.571
14	81.38	0.19	30.00	0.03	73.901	0.085	6	2.571
15	80.43	0.10	40.27	0.05	72.306	0.028	6	2.571
16	80.72	0.10	49.84	0.06	70.854	0.128	5	2.776
17	80.87	0.23	59.90	0.05	68.762	0.206	5	2.776
18	81.54	0.16	70.40	0.07	67.208	0.081	6	2.571
19	82.44	0.37	80.32	0.08	64.793	0.374	5	2.776
20	84.92	0.51	90.95	0.16	63.138	0.359	5	2.776
21	120.00	0.09	1.12	0.08	79.140	0.044	6	2.571
22	120.03	0.09	10.27	0.05	78.030	0.031	6	2.571
23	120.04	0.10	19.99	0.04	76.644	0.057	5	2.776
24	120.21	0.10	30.15	0.30	75.270	0.052	6	2.571
25	120.52	0.10	40.09	0.04	73.717	0.083	6	2.571
26	120.92	0.13	50.05	0.05	72.184	0.107	5	2.776
27	123.41	0.54	60.60	0.54	70.482	0.150	5	2.776
28	121.22	0.19	71.60	0.50	68.127	0.101	5	2.776
29	122.63	0.31	80.76	0.17	66.521	0.099	5	2.776
30	124.61	0.50	91.11	0.12	64.515	0.116	6	2.571

Table A.3: Measurements for ASTM seawater

Sl. No.	$\overline{S}$ (g/kg)	$u_{c\overline{S}}$ (g/kg)	$\overline{T_b}$ °C	$U_{\overline{T_b}}$ °C	$\overline{\gamma}$ (mN/m)	$U_{\overline{\gamma}}$ (mN/m)	n	k
1	20.19	0.09	0.78	0.28	76.098	0.087	5	2.776
2	20.17	0.10	9.92	0.19	74.802	0.061	5	2.776
3	20.01	0.09	19.90	0.09	73.389	0.102	5	2.776
4	20.04	0.09	30.00	0.09	71.805	0.087	5	2.776
5	20.10	0.09	40.17	0.20	70.195	0.178	5	2.776
6	20.23	0.10	50.45	0.16	68.555	0.148	4	3.182
7	20.41	0.10	60.45	0.05	66.807	0.081	5	2.776
8	20.26	0.10	70.89	0.15	64.932	0.077	5	2.776
9	20.57	0.11	80.43	0.25	63.121	0.170	5	2.776
10	21.20	0.13	90.51	0.08	61.344	0.177	5	2.776
11	35.47	0.09	1.23	0.13	76.389	0.120	5	2.776
12	35.47	0.09	10.05	0.04	75.033	0.174	5	2.776
13	35.28	0.11	20.92	0.03	73.477	0.140	5	2.776
14	35.20	0.09	30.03	0.03	72.257	0.094	5	2.776
15	35.38	0.10	39.85	0.03	70.562	0.202	5	2.776
16	35.54	0.21	49.73	0.04	69.091	0.159	5	2.776
17	35.85	0.11	59.46	0.08	67.592	0.112	5	2.776
18	35.48	0.10	72.36	0.22	65.170	0.076	5	2.776
19	36.36	0.15	79.50	0.03	63.717	0.117	5	2.776
20	37.64	0.27	90.02	0.19	61.889	0.196	5	2.776
21	40.79	0.09	2.88	0.12	76.425	0.094	5	2.776
22	40.78	0.09	10.37	0.03	75.361	0.167	5	2.776
23	40.53	0.10	19.99	0.08	73.871	0.051	5	2.776
24	40.52	0.09	29.98	0.06	72.516	0.094	5	2.776
25	40.61	0.09	40.37	0.08	70.952	0.119	6	2.571
26	40.76	0.10	50.58	0.09	69.351	0.083	5	2.776
27	40.82	0.11	60.48	0.06	67.383	0.157	5	2.776
28	41.16	0.12	70.29	0.22	65.831	0.103	5	2.776
29	41.64	0.17	79.96	0.07	64.218	0.103	5	2.776
30	42.80	0.26	92.07	0.22	62.106	0.243	5	2.776
31	79.90	0.09	2.28	0.11	77.580	0.148	4	3.182
32	79.82	0.09	10.07	0.19	76.496	0.053	5	2.776
33	79.85	0.09	19.58	0.11	75.229	0.067	5	2.776
34	79.86	0.11	29.98	0.03	73.715	0.105	4	3.182
35	79.49	0.10	40.16	0.25	71.999	0.155	4	3.182
36	79.73	0.11	50.85	0.29	70.193	0.106	4	3.182
37	79.94	0.24	60.80	0.03	68.536	0.302	3	4.303
38	80.64	0.23	70.65	0.06	66.978	0.093	4	3.182
39	81.74	0.26	80.09	0.16	65.191	0.091	5	2.776
40	83.71	0.64	90.53	0.04	63.507	0.191	4	3.182

Table A.3: Measurements for ASTM seawater (continued)

Sl. No.	$\overline{S}$ (g/kg)	$u_{c\overline{S}}$ (g/kg)	$\overline{T_b}$ °C	$U_{\overline{T_b}}$ °C	$\overline{\gamma}$ (mN/m)	$U_{\overline{\gamma}}$ (mN/m)	n	k
41	121.54	0.11	2.29	0.05	78.754	0.040	5	2.776
42	121.56	0.11	9.82	0.06	77.901	0.066	6	2.571
43	122.17	0.11	19.92	0.04	76.669	0.059	5	2.776
44	121.65	0.11	30.01	0.03	75.189	0.072	5	2.776
45	121.82	0.11	40.22	0.13	73.767	0.101	6	2.571
46	122.20	0.14	51.48	0.09	72.241	0.070	5	2.776
47	122.86	0.15	60.86	0.04	70.493	0.073	5	2.776
48	123.89	0.18	71.21	0.05	68.896	0.134	7	2.447
49	126.49	0.25	80.68	0.06	67.130	0.102	5	2.776
50	130.96	0.82	87.40	0.48	66.109	0.329	4	3.182

Table A.4: Measurements for ASCS seawater

Sl. No.	$\overline{S}$ (g/kg)	$u_{c\overline{S}}$ (g/kg)	$\overline{T_b}$ °C	$U_{\overline{T_b}}$ °C	$\overline{\gamma}$ (mN/m)	$U_{\overline{\gamma}}$ (mN/m)	n	k
1	35.20	0.11	1.11	0.05	76.307	0.078	6	2.571
2	35.20	0.11	9.67	0.03	74.977	0.061	4	3.182
3	35.18	0.11	19.55	0.03	73.695	0.414	5	2.776
4	35.17	0.11	29.80	0.05	72.367	0.160	3	4.303
5	35.22	0.11	40.17	0.11	70.801	0.052	5	2.776
6	35.27	0.12	50.83	0.34	69.075	0.087	5	2.776
7	37.70	0.14	60.81	0.27	67.147	0.121	4	3.182
8	38.07	0.15	70.66	0.22	65.348	0.122	5	2.776
9	38.72	0.18	80.40	0.09	63.945	0.126	5	2.776
10	36.00	0.39	90.53	0.19	61.719	0.252	6	2.571

Bibliography

[1] Guohua Chen, Jingzeng She, Ling Guo, and Lijun Zhang. Study on the Surface Tension of Seawater. *Oceanologia et limnologia Sinica*, 25(3):306–311, 1994.

[2] Kevin W. Lawson and Douglas R. Lloyd. Membrane distillation. *Journal of Membrane Science*, 124(1):1–25, February 1997.

[3] Abdulmalik A. Alhusseini, Kemal Tuzla, and John C. Chen. Falling film evaporation of single component liquids. *International Journal of Heat and Mass Transfer*, 41(12):1623–1632, 1998.

[4] R H Fleming and Roger Revelle. Physical Processes in the Ocean. *Recent Marine Sediments*, pages 48–141, 1939.

[5] Mostafa H Sharqawy, John H. Lienhard, and Syed M Zubair. Thermophysical properties of seawater: a review of existing correlations and data. *Desalination and Water Treatment*, 16(1-3):354–380, April 2010.

[6] Karan H Mistry and John H. Lienhard V. Effect of nonideal solution behavior on desalination of a sodium chloride (NaCl) solution and comparison to seawater. In *Proc. ASME 2012 Intl. Mech. Engr. Cong. & Exp.*, IMECE2012-88261, Houston, November 2012.

[7] Koch Membrane Systems. Fluid Systems TFC-FR8" RO Element Datasheet, 2011.

[8] Ho Jung Hwang, Ke He, Stephen Gray, Jianhua Zhang, and Il Shik Moon. Direct contact membrane distillation (DCMD): Experimental study on the commercial PTFE membrane and modeling. *Journal of Membrane Science*, 371(1-2):90–98, April 2011.

[9] S.T. Hsu, K.T. Cheng, and J.S. Chiou. Seawater desalination by direct contact membrane distillation. *Desalination*, 143(3):279–287, June 2002.

[10] Bhausaheb L Pangarkar and M G Sane. Performance of air gap membrane distillation for desalination of ground water and seawater. *World Academy of Science, Engineering and Technology*, 75:973–977, 2011.

[11] Karan H. Mistry and John H. Lienhard V. Effect of Nonideal Solution Behavior on Desalination of a Sodium Chloride Solution and Comparison to Seawater. *Journal of Energy Resources Technology*, 135(4):042003, June 2013.

[12] Otto Krummel. Die Kapillaritätserscheinungen und die Oberflächenspannung des Seewassers. *Wiss. Meeresuntersuch*, 5(2):2–30, 1900.

[13] K S Spiegler and A D K Laird. *Principles of Desalination, Part B.* Number pt. 2. Elsevier Science, 2nd edition, 1980.

[14] J. D. Waals. Translation of JD Van der Waals "The thermodynamic theory of capillarity under the hypothesis of a continuous variation of density". *Journal of Statistical Physics*, 20(2):200–244, February 1979.

[15] E A Guggenheim. *Thermodynamics.* North-Holland Publishing Company, Amsterdam, 2nd edition, 1950.

[16] Paul C Hiemenz and Raj Rajagopalan. *Principles of Colloid and Surface Chemistry, revised and expanded*, volume 14. CRC Press, 1997.

[17] Lars Onsager and Nicholas N. T. Samaras. The Surface Tension of Debye-Huckel Electrolytes. *The Journal of Chemical Physics*, 2(8):528, 1934.

[18] Vladislav S. Markin and Alexander G. Volkov. Quantitative Theory of Surface Tension and Surface Potential of Aqueous Solutions of Electrolytes. *The Journal of Physical Chemistry B*, 106(45):11810–11817, November 2002.

[19] Frank J. Millero, Rainer Feistel, Daniel G. Wright, and Trevor J. McDougall. The composition of Standard Seawater and the definition of the Reference-Composition Salinity Scale. *Deep Sea Research Part I: Oceanographic Research Papers*, 55(1):50–72, January 2008.

[20] H Preston-Thomas. The International Temperature Scale of 1990(ITS-90). *Metrologia*, 27(1):3–10, 1990.

[21] J Drelich, Ch Fang, and C L White. Measurement of interfacial tension in fluid-fluid systems. In *Encyclopedia of Surface and Colloid Science*, pages 3152–3166. Marcel Dekker, Inc., 2002.

[22] P. R. N. Childs, J. R. Greenwood, and C. A. Long. Review of temperature measurement. *Review of Scientific Instruments*, 71(8):2959, 2000.

[23] T G Beckwith, R D Marangoni, and John H. Lienhard V. *Mechanical Measurements.* Pearson Prentice Hall, 6th edition, 2007.

[24] J. Safarov, S. Berndt, F. Millero, R. Feistel, A. Heintz, and E. Hassel. (p,ρ,T) properties of seawater: Extensions to high salinities. *Deep Sea Research Part I: Oceanographic Research Papers*, 65:146–156, July 2012.

[25] Mostafa H. Sharqawy. New correlations for seawater and pure water thermal conductivity at different temperatures and salinities. *Desalination*, 313:97–104, March 2013.

[26] Khurshid Ali, Salma Bilal, and Shazia Siddiqi. Concentration and temperature dependence of surface parameters of some aqueous salt solutions. *Colloids and Surfaces A: Physicochemical and Engineering Aspects*, 272(1-2):105–110, January 2006.

[27] Jiri Celeda and Stansilav Skramovsky. The metachor as a characteristic of the association of electrolytes in aqueous solutions. *Collect. Czech. Chem. Commun.*, 49, 1984.

[28] N I Gelperin. Zhutnal prikladnoi khimii. *Zhutnal prikladnoi khimii*, 42:214–216, 1969.

[29] A. Horibe, S. Fukusako, and M. Yamada. Surface tension of low-temperature aqueous solutions. *International Journal of Thermophysics*, 17(2):483–493, March 1996.

[30] M A Scheiman and N L Jarvis. Surface Potentials of Aqueous Electrolyte Solutions. *The Journal of Physical Chemistry*, 72(1):74–78, 1968.

[31] Cari S Dutcher, Anthony S Wexler, and Simon L Clegg. Surface tensions of inorganic multicomponent aqueous electrolyte solutions and melts. *The journal of physical chemistry. A*, 114(46):12216–30, November 2010.

[32] Gustav Jäger. Über die Abhängigkeit der Capillaritatsconstanten von der Temperatur und deren Bedeutung für die Theorie der Flüssigkeiten. *Sitzungsber K Akad Wissen Wien, Math-Wissen Klasse, Abt. 2a*, 100:245–270, 1891.

[33] M Knudsen. Hydrographische Tabellen, GEC Gad, Copenhagen, L. *Friedrichsen & Co., Hamburg, Buchdruckerei Bianco Luno*, 1901.

[34] IAPWS. IAPWS Release on Surface Tension of Ordinary Water Substance. Technical report, International Association for the Properties of Water and Steam, 1994.

[35] DataPhysics. *DCAT 11/DCAT 11EC Brochure.* DataPhysics Instruments GmbH, Filderstadt, Germany, 2014.

[36] DataPhysics. *Products for surface chemistry.* DataPhysics Instruments GmbH, Filderstadt, Germany, 2013.

[37] C C Chan, H Lam, and X M Zhang. Practical Approaches to Method Validation and Essential Instrument Qualification, 2011.

[38] OIML. International Recommendation OIML R 111-1 Edition 2004 (E), 2004.

[39] Sartorius AG. *Sartorius Weigh Cells Installation Instructions.* Goettingen, Germany, 2009.

[40] CTech Glass. *DC-0010-002: Crystallizing Dish, Without Spout.* CTech Glass, River Edge, NJ 07661, USA.

[41] Fluke Corporation Hart Scientific Division. *Teflon-Coated Secondary Reference Thermistor Probe.* Fluke Corporation Hart Scientific Division, American Fork, Utah 84003, 2006.

[42] Fluke Calibration. *1523 / 1524 Reference Thermometers.* Everett, Washington 98206, USA, 2012.

[43] International Standards Organization. *ISO/IEC 17025: General requirements for the competence of testing and calibration laboratories.* 2005.

[44] NCSL. ANSI NCSL Z540.1 1994, 2002.

[45] Julabo USA Inc. *F12-ED Refrigerated/Heating Circulator.* Allentown, PA 18109, USA, 2014.

[46] Mettler Toledo. *Mettler Toledo AG204 Delta Range.* Columbus, OH 43240, USA.

[47] Mettler Toledo. *Mettler Toledo PG2002-S.* Columbus, OH 43240, USA.

[48] Ohaus Corporation. *Ohaus Scout II SC2040.* Parsippany, N.J., USA.

[49] Sigma-Aldrich. *ACS reagent Water.* St. Louis, MO 63103, USA.

[50] ASTM International. *ASTM D1141-98(2008) Standard Practice for the Preparation of Substitute Ocean Water.* ASTM International, 2008.

[51] OSIL. *Atlantic Seawater Conductivity Standard.*

[52] OSIL. *Preparation and Calibration of IAPSO Seawater Standard.* 2014.

[53] Sigma-Aldrich. *5M BioUltra sodium chloride solution.* St. Louis, MO 63103, USA.

[54] Ricca Chemical Company. *ASTM D 1141 Substitute Ocean Water, without Heavy Metals.* Arlington, TX 76012, USA.

[55] BUCHI Labortechnik AG. *R-210 Rotovapor with V-850 Controller.* Flawii, Switzerland.

[56] Millipore. *Milli-Q Academic A10.* Billerica, MA, USA, 2014.

[57] Kimberely-Clark Professional. *Kimwipes delicate task wipes.* Roswell, GA 30076, USA.

[58] Jack Philip Holman and Walter J Gajda. *Experimental Methods for Engineers*, volume 2. McGraw-Hill Nueva York, 7th edition, 1994.

[59] Bureau Internatinal des Poids et Mesures. Evaluation of measurement data Guide to the expression of uncertainty in measurement. Technical Report September, BIPM, 2008.

[60] Gregory Patience. *Experimental Methods and Instrumentation for Chemical Engineers*. Elsevier, 1st edition, 2013.

[61] A A Abramzon and R D Gaukhberg. Surface Tension of Salt Solutions. *Russian Journal of Applied Chemistry*, 66(8):1473–1480, 1993.